American Mineralogist, Volume 104, pages 348–369, 2019

Review

Composition, paragenesis, and alteration of the chevkinite group of minerals

Ray Macdonald[1,2], Bogusław Bagiński[1,*], Harvey E. Belkin[3], and Marcin Stachowicz[1]

[1]Institute of Geochemistry, Mineralogy and Petrology, University of Warsaw, 02-089 Warszawa, Poland
[2]Environment Centre, Lancaster University, Lancaster LA1 4YQ, U.K.
[3]11142 Forest Edge Drive, Reston, Virginia 20190-4026, U.S.A.

Abstract

The chevkinite-group minerals (CGM) are dominantly monoclinic REE-Ti-Fe sorosilicates [$(REE, Ca)_4Fe^{2+}(Fe^{2+},Fe^{3+},Ti)_2Ti_2(Si_2O_7)_2O_8$)], with REE_2O_3 contents up to ~50 wt%, but members with predominant Mg, Al, Mn, Cr, Sr, or Zr in one of the cation sites are also known. Twelve members have been approved by the Commission of New Minerals, Nomenclature and Classification International Mineralogical Association (CNMNC-IMA) but more will undoubtedly be identified. Minerals of the group are known from hundreds of terrestrial localities and have also been recorded in lunar and martian rocks. The main occurrences are in igneous rocks ranging from diamond in kimberlites through mafic and intermediate lithologies to metaluminous and peralkaline felsic rocks. They also occur in metamorphic rocks, including granulites, metacarbonates, and jadeitites, and in metasomatic rocks, such as skarns and fenites, and in rare-metal deposits. Chevkinite-group minerals may form over the pressure range 50 to <10 kbar, and over a wide temperature range. Their formation appears to be relatively insensitive to P_{H_2O} and f_{O_2}.

The stability of CGM vis-à-vis other REE-Ti-bearing accessories is poorly understood. They are often the major carriers of REE and actinides, and they have a high potential for fractionating the light lanthanides and Th from U. Very little systematic work has been done in determining CGM-melt partition coefficients, yet such data are critical in, *inter alia*, geochemical modeling. Similarly, CGM are amenable to geochronology due to their high Th abundances, commonly at the several percent level. In common with other REE-bearing accessories, CGM are prone to alteration by hydrothermal fluids. The nature and extent of the alteration are primarily determined by the composition of the fluids. Fluids poor in ligands tend to generate a Ti-enriched phase whose nature is unknown but is probably amorphous. With increasing $F + CO_2$ levels, complex replacement assemblages are formed, usually in more than one step. Although observational evidence of the effects of alteration and element mobility is accumulating and chemical equations can be constructed to approximate the reactions, there is still no firm geochemical basis for understanding element redistribution during these processes.

Keywords: Chevkinite-group, structure, composition, occurrence, alteration, petrogenetic significance

Introduction

The minerals of the chevkinite group are commonly regarded as rare accessory phases. Why, then, do they merit a review?

(1) Chevkinite-group minerals (CGM) occur in a very wide range of crustal environments, including igneous lithologies ranging from mafic to felsic, granulites and gneisses, hydrothermal and pegmatitic rocks, and skarns and ore deposits. Members of the group are known from hundreds of localities worldwide and hundreds more undoubtedly remain to be documented. Occurrences in mantle rocks have been reported and the group has also gone extraterrestrial: a CGM has been found in lunar basalts (Muhling et al. 2014), and Liu and Ma (2015) and Liu et al. (2015, 2016) reported two chevkinite group members in a benmoreite/trachyandesite clast in a martian breccia meteorite.

While CGM are, in many cases, a minor component of their host rocks, in other cases they are relatively abundant. For example, Vlach and Gualda (2007) found CGM to be the dominant rare earth element (REE)-bearing phase in several A-type granite intrusions of the Graciosa Province, Brazil, and Macdonald et al. (2013) reported CGM as the most important REE-bearing phases in many Paleogene granites of the Scottish and Northern Irish sections of the North Atlantic Igneous Superprovince. Padilla and Gualda (2016) recorded that of the accessory minerals in the rhyolitic Peach Spring Tuff, southwest U.S.A. (titanite, chevkinite, zircon, and apatite), chevkinite played the dominant role in the partitioning of the light rare-earth elements (LREE: La-Sm). In contrast to those examples, CGM are apparently not present in the numerous major REE-deposits of Australia, according to the compilation of Hoatson et al. (2011).

(2) A total of 55 elements have been recorded in CGM, in amounts ranging from parts per million to tens of weight percent; for comparison, the total is slightly more than the 52 recorded in the apatite supergroup by Hughes and Rakovan (2015). There

* E-mail: B.Baginski1@uw.edu.pl

0003-004X/19/0003–348$05.00/DOI: https://doi.org/10.2138/am-2019-6772

is, therefore, considerable compositional diversity, resulting in many substitution schemes and structural varieties.

(3) The range of host lithologies attests to the remarkable range of temperature and pressure conditions under which the CGM may form. A CGM found as inclusions in diamond in a kimberlite at Ranch River, Zimbabwe, grew under mantle *P-T* conditions (Kopylova et al. 1997a, 1997b). No robust estimates of the lower temperature conditions of natural CGM crystallization have been made, but their occurrence in amygdales in lavas and miarolitic cavities in intrusions points to temperatures perhaps as low as 350 °C at very low pressures.

(4) Like many REE-bearing accessory minerals, CGM are prone to metasomatic alteration, which is the introduction and/or removal of chemical components through the interaction of the host rock with fluids. With REE_2O_3 contents up to ~50 wt% and lesser, but significant, abundances of the high field strength elements (HFSE) and actinides, they can contribute to significant element mobility during metasomatism and ultimately to the origin of rare-metal ore deposits.

(5) As a result of their high Th concentrations, there is considerable potential for the CGM to be used in geochronology. Vasquez (2008) showed that for young chevkinite (<350 ka), the compositional variations in single crystals could be linked to absolute age through ^{238}U- and ^{230}Th-dating via ion microprobe analysis. An advantage is the slow diffusion rates for Th and U in comparison with other large cations, estimated as 10^{-27} and 10^{-28} m^2/s, respectively (Vasquez et al. 2014), which means that CGM dates derived from ^{238}U-^{230}Th disequilibrium are likely to be crystallization rather than cooling ages.

(6) Where CGM occur as phenocrysts in volcanic rocks or as early crystallizing phases in plutonic rocks, they can have an important influence on trace-element partitioning between melt and crystals and thus on melt fractionation paths (Green and Pearson 1988). As noted below, a few studies have determined melt/crystal partition coefficients, but little is yet known about how the partitioning varies with bulk-rock composition, *P*, *T*, and fluid composition. Chevkinite-group minerals may also act as refractory phases during partial melting of crustal rocks and retain the REE, HFSE, and actinides that might otherwise be removed in a melt or fluid phase (Green and Pearson 1988).

(7) The last three decades have seen an exponential increase in the use of REE in diverse aspects of modern technology, such as in permanent magnets for vehicle motors and wind generation, high-density batteries, phosphors for screens and lighting, and medical image contrast media (e.g., Haque et al. 2014; Dickson 2015). This greatly increased use, coupled with the near monopoly on REE production held by the People's Republic of China, has led to much REE exploration worldwide. For example, Canada wanted to have 20% of the global REE market by 2018 (Els 2014). Although CGM have not been described as the main REE carrier in any deposit, they may be present in the REE ore (e.g., Li and Zhou 2017). Thus, knowledge of CGM chemistry and petrogenesis will be important for beneficiation and exploration.

The specific aims of the review are to: (1) heighten awareness of the CGM (cf. Bagiński and Macdonald 2013); (2) describe progress in establishing their compositional range; (3) describe the crystal structure and how it varies with chemical composition; (4) outline the range of lithologies and *P-T-X* conditions in which CGM form; (5) describe compositional changes during hydrothermal alteration; (6) explore selected aspects of their petrogenetic significance; and (7) make suggestions about fruitful future lines of research on the group.

Members and structural formulas of the chevkinite group

The most widely used formula for the CGM is $A_4BC_2D_2(Si_2O_7)_2O_8$, where the common cations in each site are: A, REE, Y, Ca, Sr; B, Fe^{2+}; C, Fe^{2+}, Fe^{3+}, Mn, Ti, Al, Zr, Mg; and D, Ti (Ito and Arem 1971). Other formulations have, however, been used, e.g., $A_2B_2M_5(Si_2O_7)_2O_8$ (Chukanov et al. 2012a, 2012b), and work on new species has commonly shown that the standard formula and site allocations are not always applicable. Some workers, e.g., Sokolova et al. (2004) and Chukanov et al. (2012a), have preferred a more rigorous approach to classification, using cation allocations to specific sites on the basis of site properties, such as size and coordination number. In these approaches, up to four M sites replace the B, C, and D site terminology. Here the traditional names for sites from the simplified formula are used. The A site is occupied mainly by large REE, Ca, and Sr ions, and B, C, and D by cations of octahedral MO_6 coordination. In the asymmetric unit of the perrierite-type structure, there are two A sites (A1 and A2), one B site, one C site, and one D site. In chevkinite, the D site splits into D1 and D2. The unique sites B, C, D1, and D2 correspond to sites M1–M4 (Popov et al. 2001; Sokolova et al. 2004: Holtstam et al. 2017) and to B, C1, C2A, and C2B (Yang et al. 2002, 2007; Li et al. 2005; Xu et al. 2008).

The two most abundant members of the group are chevkinite and perrierite, which are structurally different. Haggerty and Mariano (1983) reported a robust method to discriminate between the two phases by measuring the monoclinic β angle (chevkinite ~100°, perrierite ~113°). The CGM could then be divided into the chevkinite and perrierite subgroups (Sokolova et al. 2004). We appreciate that the use of subgroups is not recommended by the CNMNC-IMA but it has proved immensely useful in descriptive studies of the CGM and will continue to do so until a committee is set up to formulate a set of nomenclature rules for the group.

The majority of chevkinites and perrierites are completely metamict and cannot, therefore, be distinguished by crystal structure. Macdonald and Belkin (2002) and Macdonald et al. (2009) found that a simple compositional feature, the relative proportions of FeO* (total Fe as Fe^{2+}) and (CaO+SrO), matched the division based on the β angle almost perfectly: Subsequently, the type perrierite-(La) was found to plot just above their suggested boundary line but could be accommodated by a slight shift of the line (Fig. 1a). While empirical, the classification scheme has proved useful in electron microprobe studies where crystal size and/or the metamict nature have precluded structural determinations. However, it will be shown below that there are ways of crossing the empirical boundary, almost certainly without structural modification.

Twelve members of the CGM have been approved to date by the CNMNC-IMA, six in the chevkinite subgroup and six in the perrierite subgroup, their formulas pointing to variable cation occupancy of the "standard" sites (Table 1). The chemical

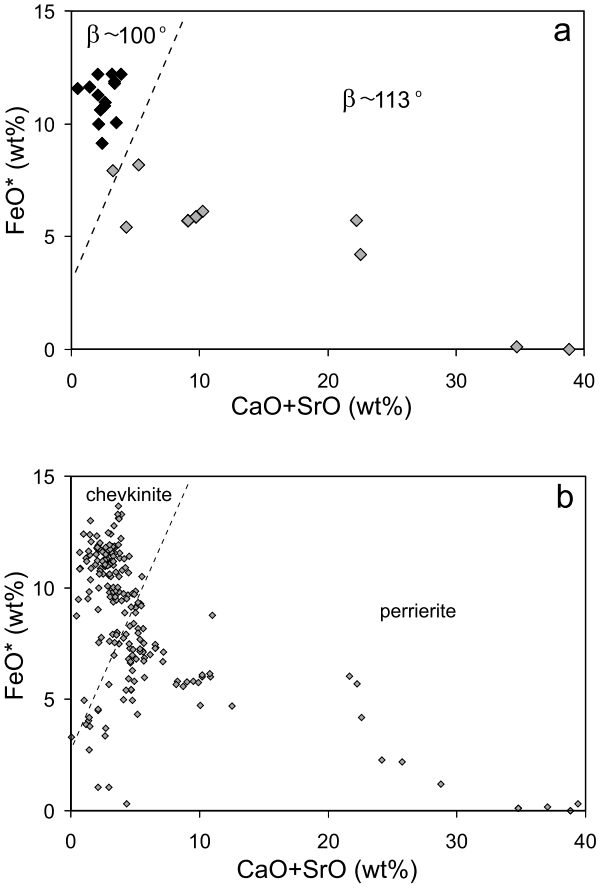

FIGURE 1. (**a**) The (CaO+SrO) – FeO* (all Fe as Fe^{2+}) plot used as an empirical discriminant between the chevkinite and perrierite subgroups by Macdonald and Belkin (2002) and modified by Macdonald et al. (2009). Data plotted are for crystals that have had the β angle determined, updated with post-2009 data. The Cr- and Mn-analogs of chevkinite-(Ce), polyakovite, and christofschäferite, respectively, are omitted. Data sources: Supplemental[1] Table S1, this paper; Jaffe et al. 1956; Gottardi 1960; Segelstad and Larsen 1978; Zhang and Long 1987; Čech et al. 1988; Imaoka and Nakashima 1994; Parodi et al. 1994; Della Ventura et al. 2001; Yang et al. 2002; Sokolova et al. 2004; Yang et al. 2008; Miyawaki et al. 2012; Stachowicz et al. 2014. (**b**) All analyses from the data compilation in Supplemental[1] Table S3 to show the wide spread of compositions across the fields of the chevkinite and perrierite subgroups.

compositions of the type minerals are listed in Supplemental[1] Table S1. Given the wide range of potential host rocks and *P-T* environments, and the flexibility of the CGM structure, it is likely that further new phases will be documented, such as Sc-dominant chevkinite, Th-dominant chevkinite, and Mg-dominant perrierite.

Certain issues concerning the nomenclature of the CGM need to be addressed at this stage. First, which sites should be used to distinguish species within the group? For example, conventional usage has been that the dominant cation in the C site in chevkinite and perrierite can be Fe or Ti. However, Xu et al. (2008) proposed that minerals with the ideal end-member composition $Ce_4Fe^{2+}Ti_2Ti_2(Si_2O_7)_2O_8$ be named dingdaohengite-(Ce), a proposal accepted by the CNMNC-IMA. Should all chevkinite with Ti dominant in the C site be renamed dingdaohengite? In the type perrierite-(Ce), from Nettuno, Italy, Al is dominant in the C site (Macdonald et al. 2009), which might preclude all perrierites with Fe or Ti dominance in the site being termed perrierite. If it is assumed that A = Ca, Sr, Y, La, Ce, Nd, Th; B = Mg, Mn, Fe^{2+}; C = Al, Ti, Cr, Fe^{2+}, Fe^{3+}, Zr, Nb; D = Ti, Nb; 294 potential combinations of site dominance could possibly be used in classification, probably not a desirable situation.

Second, knowledge of the Fe^{2+}/Fe^{3+} ratios in a phase may be important in classification. Determination by instrumental methods, such as Mössbauer spectroscopy, or by wet-chemical methods is seldom possible because of small crystal size. The ratio is often calculated from stoichiometry but such methods are influenced by the presence of non-determined elements and by analytical imprecision for elements in low abundance: Macdonald and Belkin (2002) found poor agreement in CGM between ratios calculated from stoichiometry and those determined by wet chemical methods or Mössbauer spectroscopy. As a further example, an electron microprobe analysis by Macdonald et al. (2009) of the type perrierite-(Ce) from Nettuno gave the formula $A_{4.1}BC_{1.9}D_{2.0}(Si_2O_7)_2O_8$, where all Fe was presented as Fe^{2+} and the sum of cations was 13.0. The formula is close to stoichiometric and there is apparently no need for Fe^{3+} in the phase. However, our unpublished Mössbauer spectroscopic data for the analyzed material indicates an oxidation ratio $[Fe^{3+}/(Fe^{3+}+Fe^{2+})]$ of 0.39.

The issue of an accurate knowledge of oxidation ratio is particularly important where Fe^{3+} proves to be the dominant cation in a particular site and could thus have an influence on mineral classification. Cation entry into the B site of an Fe-rich chevkinite-(Ce) from Mianning County, Sichuan, China, was given by Yang et al. (2002) as $(Fe^{3+}_{0.29}Ti_{0.21}Fe^{2+}_{0.18}Mn^{2+}_{0.13}Mg_{0.08}\square_{0.11})_{\Sigma 1.00}$.

TABLE 1. Members of the chevkinite group accepted by the CNMNC-IMA

Mineral	Formula	Reference
	Chevkinite subgroup	
Chevkinite-(Ce)	$(REE,Ca)_4Fe^{2+}(Ti,Fe^{3+},Fe^{2+},Al)_2Ti_2Si_4O_{22}$	Ito and Arem 1971
Polyakovite-(Ce)	$(REE,Ca)_4(Mg,Fe^{2+})(Cr,Fe^{3+})_2(Ti,Nb)_2Si_4O_{22}$	Popov et al. 2001
Maoniupingite-(Ce)	$(REE,Ca)_4(Fe^{3+},Ti,Fe^{2+},\square)(Fe^{3+},Fe^{2+},Nb,Ti)_2Ti_2Si_4O_2$	Shen et al. 2005
Dingdaohengite-(Ce)	$Ce_4Fe^{2+}Ti_2Ti_2(Si_2O_7)_2O_8$	Xu et al. 2008
Christofschäferite-(Ce)	$(Ce.La,Ca)_4Mn(Ti,Fe^{3+})_3(Fe^{3+},Fe^{2+},Ti)(Si_2O_7)_2O_8$	Chukanov et al. 2012b
Delhuyarite-(Ce)	$Ce_4Mg(Fe^{3+}_2W)\square(Si_2O_7)_2O_6(OH)_2$	Holtstam et al. 2017
	Perrierite subgroup	
Perrierite-(Ce)	$(REE,Ca)_4Fe^{2+}(Ti,Fe^{3+},Fe^{2+},Al)_2Ti_2Si_4O_{22}$	Ito and Arem 1971
Strontiochevkinite	$(Sr_2[La,Ce]_{1.5}Ca_{0.5})_4Fe^{2+}_{0.5}Fe^{3+}_{0.5}(Ti.Zr)_4Si_4O_{22}$	Haggerty and Mariano 1983
Rengeite	$Sr_4ZrTi_4Si_4O_{22}$	Miyajima et al. 2001
Matsubaraite	$Sr_4Ti_5(Si_2O_7)_2O_8$	Miyajima et al. 2002
Hezuolinite	$(Sr,REE)_4Zr(Ti,Fe^{3+},Fe^{2+})_2Ti_2O_8(Si_2O_7)_2$	Yang et al. 2012
Perrierite-(La)	$(La,Ce,Ca)_4(Fe^{2+},Mn)(Ti,Fe^{3+},Al)_4(Si_2O_7)_2O_8$	Chukanov et al. 2012a

Analytical totals were low (92.84–94.23 wt%) and structural water was invoked to achieve charge balance. Unusually in the CGM, vacancies in the structure were also invoked. The phase has clearly been affected by secondary hydration, with an increase in the oxidation ratio, as noted by Vlach and Gualda (2007).

In the face of these complications, formulas have been calculated here on the basis of 22 O atoms and, given the small number (13) of available Mössbauer determinations (Supplemental[1] Table S2), and uncertainties in recalculation schemes, all Fe has been taken to be Fe^{2+}. For species approved by the CNMNC-IMA the formal names are used here (Table 1). All other analyses have been classified using the empirical scheme of Macdonald et al. (2009).

Structure of chevkinite-group minerals

Part of the difficulties in determining the structure of CGM lies in the multivalent nature of cations in certain crystallographic sites, e.g., Fe^{2+}, Al^{3+}, Ti^{4+}, and Nb^{5+} in the C site. A further complication is that certain cations, importantly Fe, may exist in more than one valency state: Stachowicz et al. (2019), for example, have argued that Ti occurs as Ti^{4+}, Ti^{3+}, and possibly Ti^{2+} in Nb-rich chevkinite-(Ce) from the Biraya deposit, Mongolia. Another difficulty in comparing CGM structures is due to the use of different choices for the origin of the unit cell in part of the structures (a shift by the vector [0, 0, ½]); see below. To clarify which site in the crystal structure corresponds to a site from the empirical formula, the published data for CGM are summarized based on the nomenclature scheme used here (Supplemental[1] Table S2).

There can also be discrepancies in the assignment of cations to particular B, C, and D sites because CGM occur in different polymorphic forms, the $C2/m$ and $P2_1/a$ space groups. Stachowicz et al. (2019) noted that annealing of metamict CGM can lead to a slightly different crystal structure from the initial structure and to the migration of cations to different crystallographic sites.

It was noted earlier that chevkinite and perrierite are distinguished by different monoclinic β angles (~100° and ~113°, respectively). These are associated with a different stacking order of sheets consisting of REE cations (Stachowicz et al. 2014). The arrangement of the remaining cations for both subgroups is essentially the same, consisting of sheets of MO_6 (C and D sites) octahedra interleaved with layers of $n[B(Si_2O_7)]$ hetero-polyhedra (Calvo and Faggiani 1974). CO_6 edge-sharing octahedra form chains that share a corner with chains of DO_6 edge-sharing octahedra. Each Si_2O_7 group is joined to six BO_6 octahedra (Fig. 2). A-cations fill large cavities within the framework and are arranged in planar hexagonal arrays, with a Si-centered tetrahedron (Figs. 2 and 3) inside each array.

The green planes were plotted on two adjacent REE surfaces in both structure types to emphasize the differences in the mutual organization of REE atoms, which are the source of the different β angles of the unit cells in the two structures. Stachowicz et al. (2014) proposed that a characteristic feature of the perrierite-type structure, a D/M(3) cation displacement parallel to the tetrad axis of the coordination octahedron, is an effect of the REE stacking arrangement. A trigonal distortion of BO_6 octahedra is present in both structure types; four B-O bonds are elongated with a length of 2.2 Å and the remaining two are 2.0 Å. The C-O and D-O bond lengths in chevkinite and D-O bond lengths in perrierite are similar and within 1.9–2.0 Å.

Assuming a value of 3 Å as a limit for the A-site coordination sphere, its number varies with the space group. A-coordination polyhedra in the $C2/m$ space group have the following numbers: ^{VIII}A1 and ^{X}A2 in perrierite (Miyajima et al. 2002; Yang et al. 2012) and chevkinite (Popov et al. 2001; Yang et al. 2002, 2007; Sokolova et al. 2004). In the $P2_1/a$ space group the numbers are ^{IX}A1 and ^{IX}A2 in perrierite (Calvo and Faggiani 1974; Miyawaki et al. 2002; Chukanov et al. 2012a) and chevkinite (Calvo and Faggiani 1974; Xu et al. 2008). Stachowicz et al. (2019) found these trends in natural Nb-rich chevkinite-(Ce), one with a $C2/m$ space group and the other with $P2_1/a$. Moreover, with transformation due to annealing from $C \rightarrow P$ of a particular crystal a change in coordination numbers ^{XIII}A1 → ^{IX}A1 and ^{X}A2 → ^{IX}A2 was also observed, which is associated with a bending of the Si-O-Si angle in sorosilicate groups. The exceptions are perrierite-(Ce) with $C2/m$ and ^{IX}A1 and ^{IX}A2 (Gottardi 1960) and delhuyarite-(Ce) with $C2/m$ and ^{VIII}A1 and ^{XII}A2 (Holtstam et al. 2017). The only CGM member with the $P2_1/m$ space group, christofschäferite-(Ce), has four independent A sites in the asymmetric unit, ^{VIII}A1, ^{X}A2, ^{VIII}A3, and ^{X}A4 (Chukanov et al. 2012b).

Status of dingdaohengite-(Ce) and maoniupingite-(Ce)

The status of the Fe-Ti-dominant phases maoniupingite-(Ce) (Shen et al. 2005) and dingdaohengite-(Ce) (Xu et al. 2008; Kasatkin et al. 2015) is unclear, in particular their relationship

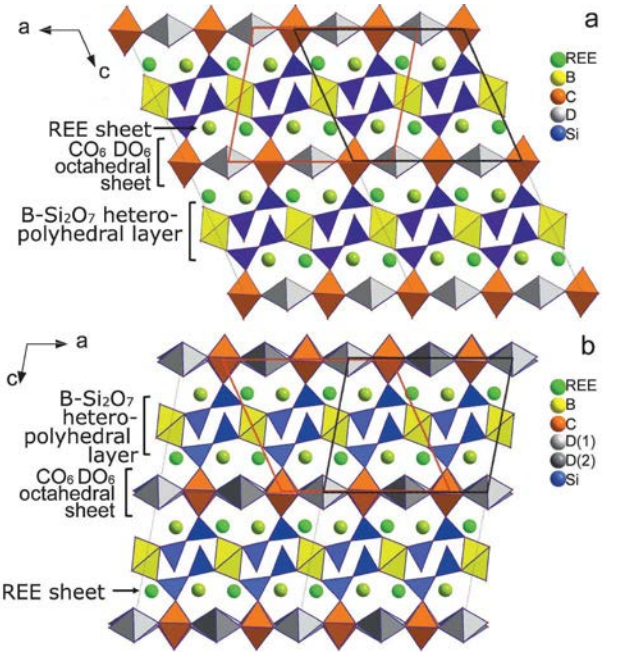

Figure 2. The 010 projection of a 2 × 2 multiplied lattice cell of (**a**) perrierite-type structure and (**b**) chevkinite-type structure. Each projection contains bold black lines representing the real unit cell of the crystal structure and bold red lines representing the unit cell of the other subgroup type. (Color online.)

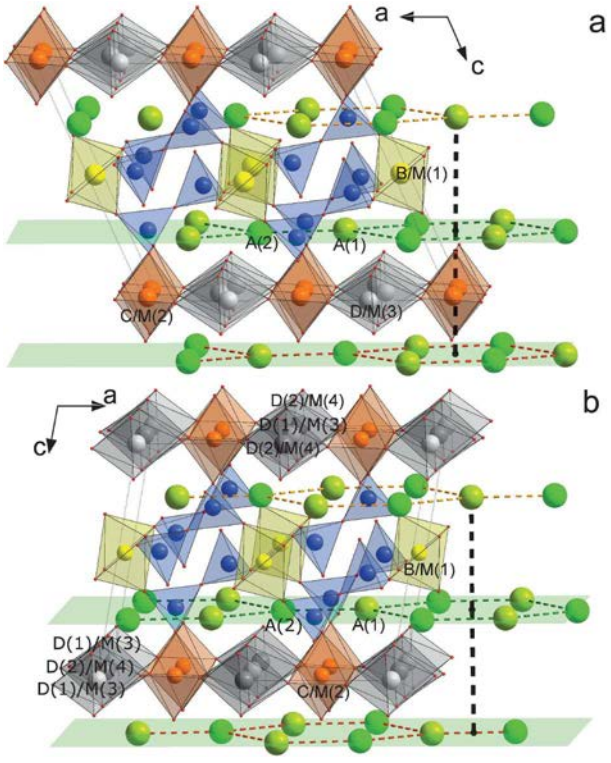

FIGURE 3. The unit-cell contents of (**a**) perrierite and (**b**) chevkinite, with an additional (lowermost green) sheet of REE. This plane is displaced by the vector [0 ½ 0] when comparing the two structure types—see broken-off bond. It ends in the middle of an REE hexagon in perrierite (**a**) and between two REE atoms in chevkinite (**b**). (Color online.)

to chevkinite-(Ce) (Belkin et al. 2009). Xu et al. (2008) assigned Fe^{2+} to the B/M1 and C/M2 sites; however, the corresponding deposited crystal structure cif file contains different information. Xu et al. (2008) placed the origin of the unit cell in their crystal structure in a different position relative to their reference structure determined by Sokolova et al. (2004). Xu et al. (2008) also exchanged the B/M1 and D2/M4 sites in their crystal structure. The error came from a comparison of identical fractional coordinates to those of Sokolova et al. (2004), despite their different Wyckoff positions. Moreover, although the C/M2 site is assigned correctly there are two crystal information files (cif) available, one in the one in the American Mineralogist Crystal Structure Database (AMCSD, http://rruff.geo.arizona.edu/AMS/amcsd.php, cif reference code 0014198) and one in the Inorganic Crystal Structure Database (ICSD, cif reference code 157061). The occupancies for the C sites are different in the two files, 23.2 and 21.4 assigned electron counts, yet the anisotropic displacement parameters are identical. The same applies to the D2/M4 site. In the ICSD cif the occupancy is 0.84 Fe, in the AMCSD cif there is a full occupancy of Fe (21.8 vs. 26 electrons) yet the anisotropic displacement parameters are again identical. We recommend that the crystal structure of dingdaohengite-(Ce) be revisited, with Fe^{2+} and Mg^{2+} being assigned to the B site, which will result in electron counts close to the experimentally refined value.

Maoniupingite-(Ce) (Shen et al. 2005), first referred to as Fe-rich chevkinite-(Ce) by Yang et al. (2002), is acknowledged as a mineral species due to the dominance of Fe^{3+} in the B site. Yang et al. (2002) allocated to this site the following components: $Fe^{3+}_{0.29}Th_{0.21}Fe^{2+}_{0.18}Mn^{2+}_{0.13}Mg_{0.09}\square_{0.11}$. The ratio of $Fe^{3+}/\Sigma Fe$ = 0.61 was based only on charge distribution calculations (Nespolo et al. 1999). In later structural studies of chevkinite-(Ce) from the same locality and based on the same average of 24 electron microprobe analyses (Li et al. 2005; Yang et al. 2007) the total $Fe^{3+}/(Fe^{3+}+Fe^{2+})$ ratio, based on Mössbauer spectroscopy, was given as 0.39, which contradicted the earlier assumption from charge distribution calculations. The B site was considered to be occupied by the following cations: $Fe^{2+}_{0.61}Mn_{0.13}Ti_{0.12}Mg_{0.08}$. The experimental evidence apparently shows that maoniupingite-(Ce) should be discredited as a mineral species, instead it is chevkinite-(Ce), as suggested by Belkin et al. (2009).

Given these uncertainities, dingdaohengite-(Ce) and maoniupingite-(Ce) have not been included in the following discussion of compositional variation in chevkinite and perrierite.

COMPOSITION OF CHEVKINITE-GROUP MINERALS

Chemical compositions of CGM were collected from the literature and our unpublished data (Supplemental[1] Table S3). In our experience, an oxide total ≥96 wt% is acceptable for CGM, in that few analyses present the full range of elements, especially all the REE, Nb, Th, and Zr, and some Fe is commonly present as Fe^{3+} although all Fe is normally presented as Fe^{2+}. After application of the 96 wt% filter, the number of analyses compiled was 266, with 164 in the chevkinite subgroup and 102 in the perrierite subgroup. The nature of the data set is variable: some are averages, while others are multiple point analyses of several crystals in the same sample, especially where the compositional range in the sample was taken to be important. In places, reference is made in the text to specific analyses not included in the data set, e.g., the Th-chevkinite of Doelter (1931).

One caveat concerning the elemental composition of CGM, especially minor components, is that most published data are obtained with electron microprobe wavelength-dispersive spectroscopy that limits, or precludes, detection of elements such as B, Be, and Li. Laser ablation-inductively coupled mass spectroscopy analysis of CGM would be helpful in obtaining a more complete inventory of substituent elements.

Chevkinite and perrierite

The compositional ranges in chevkinite and perrierite (excluding Sr-rich varieties, polyakovite and delhuyarite, which are discussed separately) are given in Supplemental[1] Table S4. There are major overlaps between the subgroups for all elements. Given the nature of the compositional discriminant employed (Figs. 1a and 1b), a main difference is in the (CaO+SrO) and FeO* contents. Perrierite has higher average abundances of Al_2O_3, MgO, CaO, SrO, and ZrO_2, and lower average contents of FeO*, Nb_2O, and ΣREE_2O_3 than chevkinite. In the C site of chevkinite Fe > Ti > Al; in perrierite Ti > Al > Fe. Magnesium is required to fill the C site in many perrierite analyses but not in chevkinite. The main compositional variations are expressed in the general equation proposed by Vlach and Gualda (2007): $(Ca^{2+} + Sr^{2+})_A + (Ti^{4+} + Zr)_C \leftrightarrow [(REE,Y)^{3+}]_A + (M^{2+,3+})_C$ (Fig. 4).

Compositional evolution *within* the chevkinite and perrierite subgroups generally follows the trend shown in Figure 4, the

trend toward an increasingly "chevkinitic" character indicating an increasingly felsic character of the host rocks. This tendency was shown in a $\Sigma(La_2O_3\text{-}Sm_2O_3)$-FeO*-$(CaO+SrO+MgO+Al_2O_3)$ plot by Macdonald and Belkin (2002) (Fig. 5).

One consequence of the compositional trends is that some magmatic trends may cross the empirical boundary on the discriminant plot (Fig. 6). It is improbable that the structure changes (e.g., the β angle from ~113° to ~100°), especially within single crystals, as represented by the Azambre et al. (1987) example shown in Figure 6. It is more likely that there is a zone around the boundary where phases can exist in either structural state, as predicted by Macdonald and Belkin (2002). As Muhling et al. (2014) stressed, structural study is required to determine precisely the nature of phases in the transitional zone. Nevertheless, the discriminant has proven to be a useful tool in CGM studies, allowing preliminary names to be given to phases where no structural study has been possible.

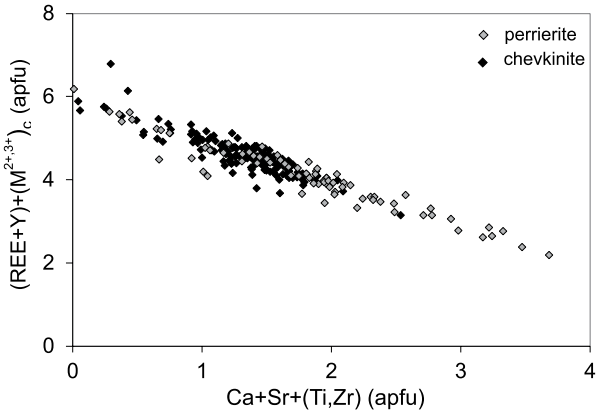

FIGURE 4. The main compositional variation in chevkinite and perrierite, using the scheme of Vlach and Gualda (2007). Sr-rich varieties of perrierite, polyakovite and christofschäferite omitted. The perrierites with values of Ca+Sr+(Ti,Zr) <1 are mainly Al-rich varieties. Data source: Supplemental[1] Table S3.

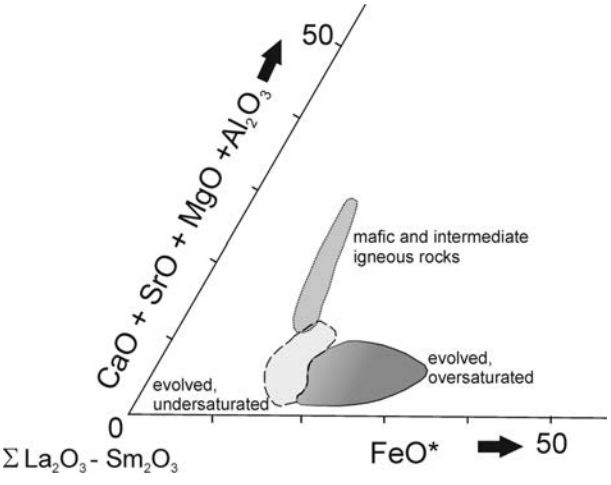

FIGURE 5. Triangular plot to show that chevkinite and perrierite tend to occur in different igneous lithologies. The fields marked "evolved, undersaturated" and "evolved, oversaturated" are occupied only by chevkinite. The field of mafic and intermediate igneous rocks includes only perrierite. Slightly simplified from Macdonald and Belkin (2002). Data gathered since 2002 have tended to blur the distinction between the two "evolved" fields.

A site

The dominant cations in the A site are REE and Ca. Rare earth elements predominate, exceptions being two point analyses from kersantites of the Oroscocha volcano, Peru, where Ca > REE (Fig. 7), potentially making the phase perrierite-(Ca). A constraint on describing REE distribution is the scarcity of complete data sets. For example, Eu concentrations have been reported in only 45 analyses (including values given as below detection). The large compositional range is, therefore, demonstrated here on a plot of $[La/Nd]_{CN}$ (as a measure of fractionation within the LREE) against $[La/Y]_{CN}$ [fractionation of LREE from heavy rare earth elements (HREE; Gd-Yb), with Y proxying for the HREE] (Fig. 8). The full data set has the following features.

(1) Ce is overwhelmingly the dominant REE in the site; La exceeds Ce in only seven cases. The type perrierite-(La) was described from the Eifel volcanic district, Germany, by Chukanov

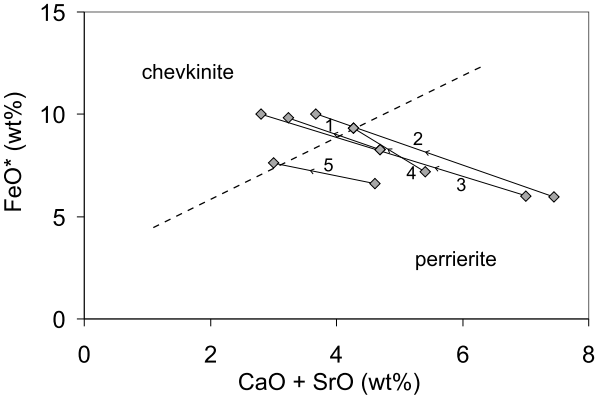

FIGURE 6. CaO+SrO – FeO* plot showing various magmatic trends crossing the empirical boundary between the chevkinite and perrierite subgroups. The arrows point in the down-temperature direction. 1 = tholeiitic dolerite, French Pyrenees (Azambre et al. 1987); 2 and 3 = Woodie and Eel Creek tholeiitic intrusions, Western Australia (Muhling et al. 2014); 4 = Little Chief porphyry stock, California (McDowell 1979); 5 = Roseland, Virginia (Macdonald et al. 2009).

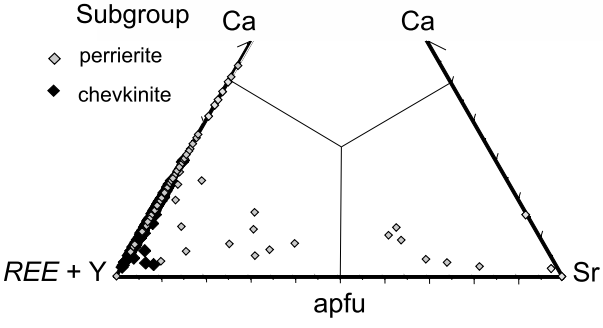

FIGURE 7. Cation distribution in the A site in CGM. Data source: Supplemental[1] Table S3.

et al. (2012a), although perrierite analyses with dominant La had earlier been reported, without structural data, from Bjørkedalen in the Oslo region, Norway (Segelstad and Larsen 1978), and Golden Lake in Ontario, Canada, and Rajasthan, India (Macdonald et al. 2009). Chevkinite with La exceeding Ce was reported from Sandefjord, Bjørkedalen, and Stokkoya, Oslo region, by Segelstad and Larsen (1978), in trachyandesites from Moravia, Czech Republic (Macdonald et al. 2017a), granites from Zhitkovichi, Belarus, by Povarennykh and Ganzeeva (1972) and without presenting an analysis from a hornfels in the Khibiny massif, Kola Peninsula, Russia, by Yakovenchuk et al. (2005). However, the species has not yet been submitted to the CNMNC-IMA. Proshchenko (1967) presented three analyses of chevkinite in albitites from eastern Siberia, with La/Ce (atomic) ratios of 2.7, 1.21, and 1.16. It would be valuable to restudy this material, to determine whether the La dominance is a function of the paragenesis or the result of an analytical problem. A quite exceptional Y-dominant perrierite was described from a quartzofeldspathic gneiss of the Archean Napier Complex, Antarctica, by Belkin et al. (2009), the only record so far of a Y-dominant mineral in the CGM. Liu and Ma (2015) and Liu et al. (2015, 2016) reported a CGM with Nd dominant in the A site from martian breccia meteorite NWA 7034, the first record of such Nd dominance.

(2) Chevkinite has slightly higher ΣREE_2O_3 (37.4–53.2 wt%; average 44.5 wt%) than perrierite (26.5–51.0 wt%; average 40.7 wt%) (Supplemental[1] Table S4) but clearly REE contents alone are insufficient to distinguish the subgroups.

(3) The great majority of analyses are LREE-enriched, with $[La/Y]_{CN}$ ranging from 2–5608 (Fig. 8). Chevkinite shows stronger LREE enrichment relative to HREE than perrierite (average $[La/Y]_{CN}$ 420 and 271, respectively). In both subgroups, there is no simple relationship between the degree of enrichment, the nature of the host rock or the paragenesis. Note, for example, the major overlaps on a La-Y plot between CGM from peralkaline rhyolites (comendites) and tholeiitic intrusions, and between CGM from potassic volcanics and the A-type Woshui syenite in the Emeishan igneous province, SW China (Fig. 9).

(4) Both subgroups show large ranges in $[La/Nd]_{CN}$, indicating significant fractionation within the LREE (Fig. 8). There is apparently no simple link between the value of the ratio and any other parameter, such as host lithology or mineral paragenesis.

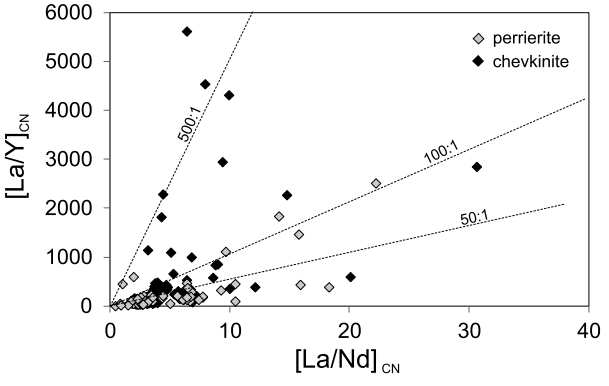

FIGURE 8. $[La/Nd]_{CN}$ (as a measure of fractionation within the LREE) vs. $[La/Y]_{CN}$ (as a measure of LREE vs. HREE fractionation).

(5) Cerium anomalies are ubiquitous and can be positive or negative, although positive anomalies are dominant (85%). The magnitude of the anomalies is similar in chevkinite (Ce/Ce* 0.6–1.4; average 1.1) and perrierite (Ce/Ce* 0.7–1.3; average 1.1). The lowest values (0.6–0.7) in both cases are predictably from the La-dominant phases from Oslofjord noted above (Segelstad and Larsen 1978).

Europium anomalies (Eu/Eu*) have been calculated for only 16 samples. Shellnutt and Iizaka (2013) recorded unusually large positive anomalies (Eu/Eu* 2.3–23) in CGM from the metaluminous Woshui syenite, noting that the anomalies mirror those in the whole rocks. Huraiová et al. (2007) reported, without comment, chevkinite-(Ce) in a syenite xenolith from the Pincina maar, Slovakia, with equally large positive anomalies (3–28). In an interesting approach, Troll et al. (2003) used an Onuma diagram to estimate the proportions of Eu^{3+} and Eu^{2+} (~33% Eu^{2+}) in chevkinite-(Ce) from Gran Canaria, Spain.

Strontium levels are very low (<0.2 apfu) in the great majority of chevkinite and perrierite analyses (Fig. 7), with the exception, *inter alia*, of perrierite-(Ce) from the Bearpaw Mountains, Montana, U.S.A. (0.35–1.18 apfu; Chakhmouradian and Mitchell 1999) and Sr-Zr-rich perrierite-(Ce) from the Burpala massif, Russia (0.88 and 0.94 apfu; Portnov 1964; Macdonald et al. 2012). Thorium abundances reach a maximum of 8.4 wt% ThO_2 (0.40 apfu) in perrierite-(Ce) from the Joe Lott Tuff Member of the Belknap Volcanics, Utah (Budding et al. 1987), an exception being a Th-rich chevkinite-(Ce) from the Urals, Russia, which has 20.9 wt% ThO_2 (Doelter 1931). Thorium abundances do not appear to be correlated with any other geochemical feature. Uranium abundances are low (≤0.30 wt% UO_2), with the exception of chevkinite-(Ce) from Samalpatti, India (2.53 wt%; Semenov et al. 1978), and Samchampi, India (0.69 wt%; Viladkar et al. 2009). Barium levels are also low, reaching 0.45–0.54 wt% BaO in chevkinite-(Ce) from syenite xenoliths in the Pinciná basaltic maar, Slovakia (Huraiová et al. 2007), although such high values may be an artifact arising from Ti uncorrected for peak interference.

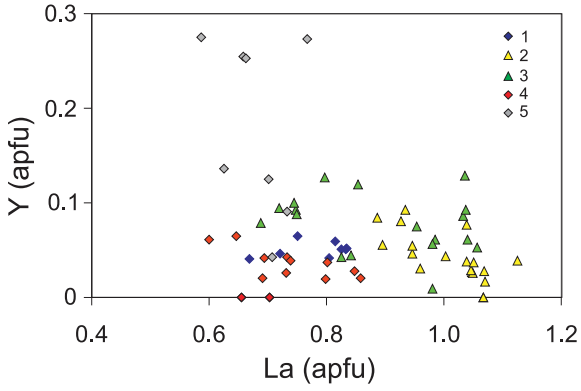

FIGURE 9. La vs.Y plot to show that the degree of LREE enrichment is not simply dependent on host rock composition. Fields: 1 = Woshui syenite, China; 2 = comendites (mildly peralkaline rhyolites); 3 = tholeiitic intrusions, Western Australia; 4 = perrierite in potassic volcanics; 5 = Al-rich perrierite, Antarctica and India. Data from Supplemental[1] Table S3 and references cited therein (Supplementary Material). (Color online.)

B site

The B site is filled in 90% of analyses by Fe^{2+}. The deficit in the remaining analyses is made up by Mn ± Mg, with the exception of a low-Fe perrierite-(Ce) from the Khibiny massif (ΣB = 0.83 apfu; Yakovenchuk et al. 2005). The Fe-deficient rocks include perrierite from Italian potassic volcanoes (Van Bergen 1984; Parodi et al. 1994; Della Ventura et al. 2001; Macdonald et al. 2009), potassic volcanics from the Oroscocha volcano (Carlier and Lorand 2008), and Al-rich perrierites from Antarctica and India (Harley 1994; Hokada 2007; Belkin et al. 2009). The latter also contains the highest levels of Mg in the B site, up to 0.77 apfu (Harley 1994), making the phase the Mg-Al-dominant analog of perrierite-(Ce).

In christofschäferite-(Ce) (Table 1) Mn fills the octahedral site B, Ti dominates the C and D2 sites, and D1 is occupied by Fe and Ti (Chukanov et al. 2012b). The phase contains 4.39 wt% MnO (0.76 Mn apfu). Povarennykh and Ganzeeva (1972) presented an analysis of chevkinite in albititized granites at Zhitkovichi, Belarus, with 5.0 wt% MnO (0.90 Mn apfu). The formula can be written as: $(La_{1.87}Ce_{1.51}Ca_{0.49}Nd_{0.17})_{4.04}(Mn_{0.90}Fe^{2+}_{0.10})(Fe^{3+}_{1.02}Ti_{0.79}Fe^{2+}_{0.21})_{2.02}Ti_{2.00}(Si_2O_7)_2O_8$, which would potentially make it the La-dominant analog of christofschäferite-(Ce).

C site

The only cations to achieve dominance in the C site are Ti, Fe^{2+}, and Al, which occur in very variable proportions (Fig. 10). Macdonald et al. (2009) listed several perrierite occurrences in Antarctica and India where Al is dominant in the site; Al-dominance in chevkinite is uncommon but has been recorded in albitites from Siberia (Proschchenko 1967) and the Pyrenees (Monchoux et al. 2006). Fe- or Ti- dominance appears not to be specific to certain lithologies; indeed both forms can be found in the same sample.

All determinations of oxidation ratio $[Fe^{3+}/(Fe^{3+}+Fe^{2+})]$ by Mössbauer spectroscopy of which we are aware are listed in Supplemental[1] Table S2. The majority are for members of the chevkinite subgroup. Values range from 0.18 to 0.61 and have no simple relationship to mineral species or to the nature of the host rock.

In the majority of point analyses the Mg levels are low (<0.3 apfu; <1 wt% MgO). The maximum Mg value recorded is 0.90 apfu (2.99 wt% MgO) in perrierite-(La) from a metacarbonate at Golden Lake, Ontario (Macdonald et al. 2009). The most consistently Mg-rich phases are Al-rich perrierites from Antarctica and Anakpalle, India (0.21–0.77 apfu; 0.72–2.74 wt% MgO; Harley 1994; Hokada 2007; Belkin et al. 2009). The majority of Mn values are low (≤0.5 wt% MnO; <0.1 apfu Mn) but there is a continuum of compositions to 0.50 apfu; then there is an apparent compositional gap to christofschäferite (1 apfu Mn).

Chromium oxide levels in chevkinite and perrierite are extremely low (≤0.13 wt%), indicating a huge compositional gap between them and polyakovite-(Ce). Scandium abundances have been reported for only seven occurrences, in only one in significant amounts, perrierite-(Ce), from Bayan Obo in Inner Mongolia, China (3.26 wt% Sc_2O_3; 0.57 apfu Sc; Shimazaki et al. 2008a). Mention may be made here of the so-called Sc-perrierite, first recorded from quartz-fluorite pegmatites in Akzhaylau, southeastern Kazakhstan by Semenov et al. (1966). Its Sc content

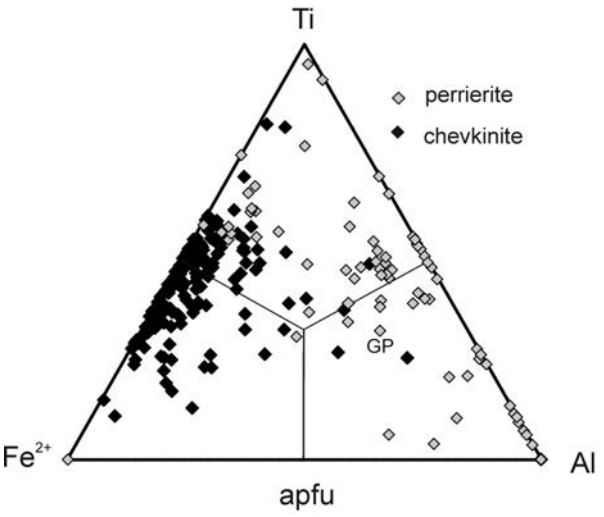

FIGURE 10. Relative proportions of Fe^{2+}-Ti-Al in the C site of minerals of the chevkinite and perrierite subgroups, excluding Sr-dominant phases, christofschäferite-(Ce) and polyakovite-(Ce). All Fe taken as Fe^{2+}. GP marks the composition of perrierite-(Ce) crystallized from REE-enriched silicate liquid at 20 kbar, *T* 1050 °C, by Green and Pearson (1988, sample 948).

was 0.82 apfu (Sc_2O_3 4.14 wt%). Scandium was thought to have entered the structure through the substitution $Sc^{3+} + Fe^{3+} = Fe^{2+} + Ti^{4+}$ and the formula given as $Ce_4ScFe^{3+}Fe^{2+}Ti_2Si_4O_{22}$. The analysis as presented has 43.3 positive charges and plots in the chevkinite field of the empirical discrimination scheme of Macdonald et al. (2009). A reinvestigation of this interesting material would be welcome. Vanadium has been reported in three samples, the highest value being 0.49 wt% V_2O_3 in perrierite-(Ce) from alkaline silicate–carbonate assemblages of the Vishnevogorsky complex, South Urals (Makagonov and Muftakhov 2016).

Niobium is commonly present in low to moderate concentrations (<5 wt% Nb_2O_5). Makarochkin et al. (1959) described, from a fenitised granite in the Ilmen Mountains, southern Urals, Russia, a phase that they named niobochevkinite. However, the phase contains only 7.4 wt% Nb_2O_5 (Nb 0.71 apfu) and is strictly Nb-rich chevkinite. Sample 10047-11 from the Moon has ~3 wt% Nb_2O_5 (Muhling et al. 2014). The most Nb-rich CGM so far recorded is from the Biraya carbonatite complex, Russia, with 11 wt% Nb_2O_5 (Stachowicz et al. 2019 and in review). Niobium is usually allocated to the C site, perhaps because in almost all chevkinites and perrierites, the D site is taken to be filled by Ti. However, Popov et al. (2001) allocated Nb to the D site in polyakovite and Stachowicz et al. (2019b) found Nb to be allocated between both C and D sites in their Nb-rich phase.

Taking 0.10 wt% as a reasonable limit of detection, 31 Ta determinations are available (Supplemental[1] Table S3), with a maximum Ta_2O_5 value of 0.50 wt% in chevkinite-(Ce) from the Paleogene Meall Dearg granite, Isle of Skye, Scotland (Macdonald et al. 2013).

Zirconium shows a fairly continuous spread of values up to 7.0 wt% ZrO_2 (0–0.63 apfu Zr). The highest values are in perrierite from the Oroscocha volcano (Carlier and Lorand 2008), in mafic sills of Western Australia, and in lunar samples

(Muhling et al. 2014). Taking 0.10 wt% as a reasonable detection limit for HfO_2, 20 determinations of Hf are available, with a maximum value of 0.44 wt% in perrierite-(Ce) from the Woshui syenite.

D site

With two exceptions, the D site is filled with Ti. Belkin et al. (2009) described two samples of perrierite-(Ce) from Antarctica with Ti and Nb abundances unable to fill the site and suggested that some Al (0.21 and 0.56 apfu) may enter the site. In their structural study of Nb-rich chevkinite from the Biraya complex, Stachowicz et al. (2019 and in review) allocated, in addition to Ti, Nb, Fe^{3+}, Fe^{2+}, and Mg to the D site.

T site

In 87% of analyses, the tetrahedral site is filled by Si. Phosphorus is sometimes considered to be a minor constituent: CGM from tholeiitic sills of Western Australia have the highest values, up to 0.062 apfu (0.37 wt% P_2O_5; Muhling et al. 2014). Huraiová et al. (2007) allocated some Al to the site (up to 0.065 apfu). Carlier and Lorand (2008) also raised the possibility of Al entering the site in perrierite-(Ce) from Oroscocha.

Anion site

Water has been reported in analyses of CGM, in amounts up to 0.90 wt% (Supplemental[1] Table S3). The question arises: did the water enter the mineral when it formed or was it added under subsolidus conditions, e.g., by hydrothermal fluids? In a study of chevkinite-(Ce) from an aegirine granite at Mianning, Yang et al. (2008) used single-crystal FTIR to detect OH in the structure, suggesting that it possibly replaced oxygen. However, their analysis gave only 42.24 positive charges; from charge balance, they calculated an OH content of 1.76 pfu (1.27 wt% H_2O). Despite this addition, the analytical total was still low (95.22 wt%), and the structural role of the OH is uncertain. More recently, Holtstam et al. (2017) recorded structural water and vacancies in delhuyarite (see below).

Fluorine has also been reported in chevkinite and perrierite, at levels up to 1 wt% (Supplemental[1] Table S3). It has been argued by Belkin et al. (2009) that the F values determined by electron microprobe represent interference between the F$K\alpha$ (λ = 18.3199 Å) and Ce-$M\xi$ (λ = 18.3499 Å) peaks. Chlorine has been recorded in four samples of chevkinite, at levels ≤0.03 wt%, possibly below a realistic detection level.

We know of no example of an absolutely pristine CGM, occurring, for example, as phenocrysts in young eruptive rocks, being shown to carry OH and F. Lacking positive evidence of these components being incorporated during crystallization, we suggest that pristine CGM are volatile free.

Polyakovite-(Ce)

Polyakovite-(Ce) was first recorded in a carbonatite (dolomite) veinlet cross-cutting a phlogopite-olivine rock in the Ilmen Mountains (Popov et al. 2001). It is an unusual member of the chevkinite group, in that Cr is a species-forming element. The structural formula is $(Ce_{1.86}La_{1.23}Nd_{0.35}Pr_{0.15}Sm_{0.01}Y_{0.04}Ca_{0.24}Th_{0.12})_{4.00}(Mg_{0.80}Fe^{2+}_{0.20})_{1.00}(Cr_{1.28}Fe^{3+}_{0.72})_{2.00}(Ti_{1.52}Nb_{0.32}\square_{0.16})_{2.00}Si_{4.00}O_{22.00}$. Magnesium is dominant at the B site [M(1) in the terminology of Popov et al. (2001)], and Cr is dominant at the C [M(3) and M(4)] sites. Also unusual is the presence of vacancies in D [M(2)]. A later analysis of a co-type from the same locality showed slightly higher Cr_2O_3 and Nb_2O_5 contents, and lower SiO_2, FeO*, MgO, CaO, and La_2O_3 contents (Macdonald et al. 2012). Their structural formula did not include vacancies.

Earlier, Kopylova et al. (1997a, 1997b) had described a mineral that they termed Cr-chevkinite, occurring as inclusions in diamonds from the River Ranch kimberlite pipe in Zimbabwe. They gave the formula as $(Ce_{2.22}La_{0.96}Nd_{0.51}Pr_{0.18}Th_{0.06}Sr_{0.29})_{3.99}(Mg_{0.46}Fe^{2+}_{0.23}Ca_{0.13})_{0.83}Cr_{1.95}(Ti_{1.44}Nb_{0.26}\ Al_{0.32})_{2.02}Si_{4.02}O_{22}$. Despite some minor differences, there are clear similarities to polyakovite-(Ce), a particular point of interest being the much higher Cr content. The inclusions in the River Ranch kimberlite may have been formed during a K-metasomatic event and incorporated into diamonds outside the diamond stability field prior to, or during, kimberlite eruption (Kopylova et al. 1997b).

Delhuyarite-(Ce)

Delhuyarite-(Ce), the newest CGM, is known from only one locality, the Nya Bastnäs Fe-Cu-REE deposit in Sweden (Holtstam et al. 2017). Its ideal formula is given as $Ce_4Mg(Fe^{3+}_2W)\square(Si_2O_7)_2O_6(OH)_2$. The W content (0.89 apfu; 15.53 wt% WO_3) is quite unique in the CGM. Also notable are the dominance of Mg in the M1 site, the presence of H_2O, confirmed by IR spectroscopy from a strong absorption band at 3495 cm^{-1}, and a 50% vacancy in the M2 site. Vacancies in the structure were invoked partly to explain the entry of W into the phase, via a charge-balanced exchange mechanism of the type: $2Ti^{4+} + 2O^{2-} \leftrightarrow W^{6+} + \square + 2(OH^-)$. The unusual nature of the phase may be related to its formation from hot (initially ≥400 °C), originally juvenile magmatic fluids (Holtstam et al. 2017).

Sr-rich varieties

These are defined here as having Sr > Ca and include, therefore, the Sr-dominant species rengeite, matsubaraite, strontiochevkinite, and hezuolinite (Table 1). Possible compositional relationships between the species are shown in Figure 11.

Rengeite $[Sr_4ZrTi_4(Si_2O_7)_2O_8]$ is compositionally variable. Two varieties, occurring in association with natrolite and analcime in jadeitites from the type area in the Itoigawa-Ohmi district, Japan (Miyajima et al. 2001; Goto et al. 2017), contain very different proportions of REE, Ca, and Sr (Fig. 7). An orthorhombic polymorph, reported as microdomains in the rengeite, contains neither Ca nor REE (Mashima et al. 2008); however, the phase has not been submitted to the CNMNC-IMA and may not be valid. Rengeite is also known from Mount Kaskasnyunchorr, Khibiny massif, occurring in an albite-anorthoclase hornfels from a large xenolith in foyaite (Yakovenchuk et al. 2005; Mikhailova et al. 2007). It contains no REE and has the highest Ca/Sr ratio so far reported in the mineral (0.16). Matsubaraite $[Sr_4Ti_5(Si_2O_7)_2O_8]$ is known only from its type locality, the same jadeitite locality as for rengeite. It can be considered as the Zr-free analog of rengeite (Miyajima et al. 2002; Miyawaki et al. 2002).

The type locality of hezuolinite $[(Sr,REE)_4Zr(Ti,Fe^{3+},Fe^{2+})_2Ti_2O_8(Si_2O_7)_2]$ is in sodic lujavrite of the Saima alkaline complex, northeastern China (Yang et al. 2012; Wu et al. 2016).

It has not been recorded elsewhere but is in some respects similar to strontiochevkinite $\{(Sr_2[La,Ce]_{1.5}Ca_{0.5})_4Fe^{2+}_{0.5}Fe^{3+}_{0.5}(Ti,Zr)_2Ti_2(Si_2O_7)_2O_8\}$ (Haggerty and Mariano 1983), except that Zr and Fe occupy different positions in the B and C sites. There is, however, a substantial compositional gap between strontiochevkinite and Sr-Zr perrierite, such that it is difficult to identify substitution schemes. A possible scheme connecting strontiochevkinite and Sr-rich perrierite-(Ce) from Pegmatite Peak in the Bearpaw Mountains, Montana (Chakhmouradian and Mitchell 1999) is $2REE^{3+} + Fe^{2+} = Ti^{4+} + Zr^{4+}$ (Fig. 11). Strontiochevkinite and Sr-Zr perrierite-(Ce) may be connected by the scheme $REE^{3+} + Fe^{2+} = Sr^{2+} + Fe^{3+}$ (Fig. 11).

Occurrence of chevkinite and perrierite

Igneous rocks

Chevkinite and perrierite have been recorded in very diverse igneous lithologies, in a range extending from ultramafic cumulates to granitic pegmatites. Mutanen (1997) reported perrierite as an intercumulus phase in ultramafic cumulates of the Akanvaara and Koitelainen mafic layered intrusions, northern Finland. It has long been recognized that CGM are common in mafic and intermediate rocks of potassic affinity. However, it is increasingly recognized that they also occur in more sodic types; Muhling et al. (2014) described CGM in tholeiitic intrusive rocks from Western Australia and Melluso et al. (2014) found CGM in low-Ti, low-Fe tholeiitic rocks from Tasmania. In the tholeiitic types, the CGM commonly occur in late-stage granophyric patches, indicating that they crystallized when the residual melts had felsic compositions.

There are some lithologies where CGM are scarce or absent, such as peraluminous granites where the main REE-bearing phase tends to be monazite. Their absence from mid-ocean ridge basalts possibly results from the low Ti and REE contents of such rocks. CGM are also relatively uncommon in *strongly* peralkaline [(mol. $(Na_2O+K_2O)/Al_2O_3 > 1.3$)] rhyolites and granites, where aenigmatite and astrophyllite tend to be the stable Ti-bearing phases. However, Noble (1965) recorded chevkinite in pantellerite of the Gold Flat Member of the Thirsty Canyon Tuff, Nevada; although he did not present an analysis we have confirmed its presence via electron microprobe analyses (unpublished data).

Early magmatic

Chevkinite-group minerals occur as (micro)phenocrysts in a wide range of lithologies, from quartz latite (Warren et al. 1989), through trachyandesites-dacites (Van Bergen 1984) and metaluminous rhyolites (Ewart 1981; Martz and Brown 1981; Cameron and Cameron 1986; Macdonald and Belkin 2002; Miyawaki et al. 2012; Vasquez et al. 2014; Padilla and Gualda 2016) to peralkaline rhyolites (Jørgensen 1980; Novak and Mahood 1986; Sawyer and Sargent 1989; Macdonald et al. 2002, 2015a; Troll et al. 2003; Marshall et al. 2009; Vasquez et al. 2014; Peretyazhko et al. 2015) (Fig. 12a).

Estimates of the temperatures and pressures of equilibration and of f_{O_2} for various CGM phenocryst occurrences have been made by different methods, including coexisting oxides, QUILF (which assesses equilibrium among T-magnetite, ilmenite, augite, pigeonite, orthopyroxene, olivine, and quartz, or subassemblages thereof), clinopyroxene-melt, $\Delta^{18}O$ (quartz-magnetite) and phase equilibrium studies, and are not strictly comparable. The temperature range is from >900 °C in quartz latites (e.g., Mills et al. 1997; Bindeman and Valley 2003) to ~700 °C in rhyolites (Mills et al. 1997; Scaillet and Macdonald 2001), with perrierite being the typical CGM at higher T and chevkinite at lower T. Pressure estimates are less well constrained but where the geological context is provided the phenocrysts can be inferred to have formed at $P \leq 5$ kbar. Oxygen fugacities vary from ΔFMQ –1 to +2 and show no simple relationship to host lithology (Mills et al. 1997; Scaillet and Macdonald 2001; Bindeman and Valley 2003; Troll et al. 2003; Macdonald et al. 2015a).

Estimates of the water contents of CGM-phyric felsic magmas generally show that such magmas were water-rich, with H_2O contents in the range 4–5 wt% (Novak and Mahood 1986; Mills et al. 1997). This is consistent with experimental evidence that chevkinite crystallized from peralkaline rhyolites (comendites) under conditions of near H_2O saturation (Scaillet and Macdonald 2001).

Also considered to be of early magmatic crystallization are CGM found as inclusions in early phases in plutonic rocks, such as feldspar, pyroxene, and amphibole (Van Bergen 1984; Ridolfi et al. 2003: Macdonald et al. 2013) (Fig. 12b). Estimates of the P-T-f_{O_2} conditions of CGM formation are broadly in line with those for phenocrysts. McDowell (1979)

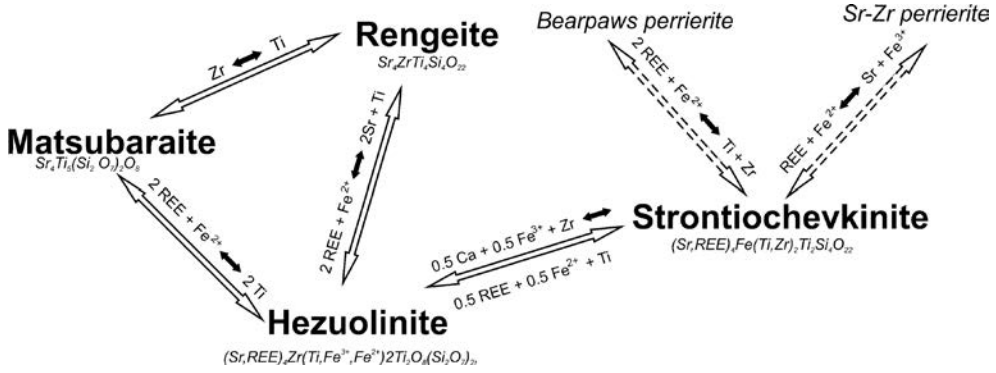

Figure 11. Graphical representation of possible substitution mechanisms in Sr-dominant perrierites (Table 1). Possible substitutions to Sr-bearing perrierite from the Bearpaw Mountains (Chakhmouradian and Mitchell 1999) and Sr-Zr perrierite, Burpala Massif (Macdonald et al. 2012) are also shown, as dashed lines.

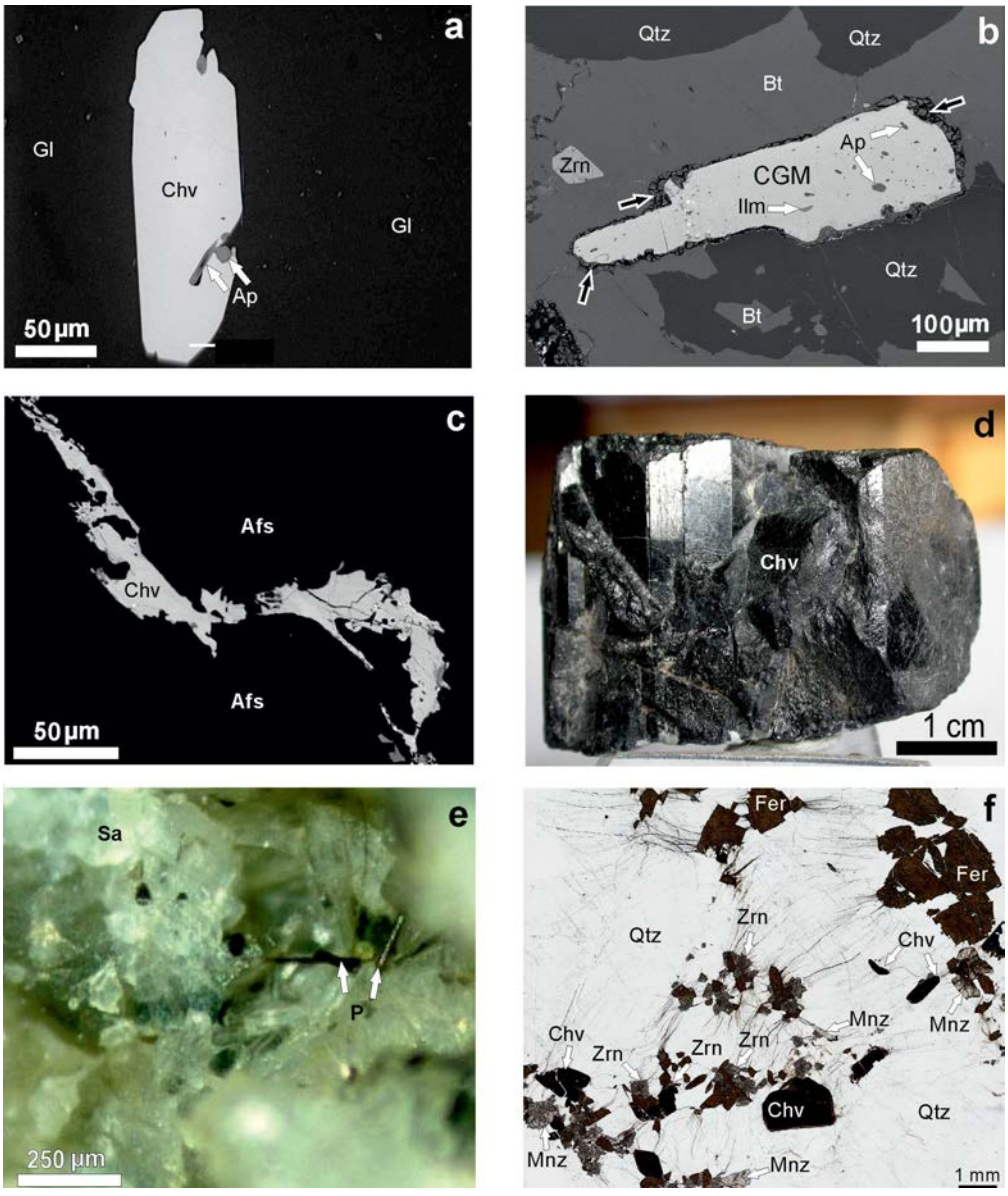

Figure 12. BSE images of CGM occurrences in igneous rocks. (**a**) Subhedral phenocryst of chevkinite-(Ce) (Chv) in comendite obsidian (glass, Gl), Olkaria complex, Kenya Rift Valley. (**b**) Associated with primary quartz (Qtz) and biotite (Bt), Lucerne Granite, Hancock County, Maine, U.S.A. Associated accessories are zircon (Zrn), ilmenite (Ilm), and LREE-bearing apatite (Ap). The crystal is surrounded by a hydrated alteration zone (black arrows). (**c**) Late magmatic chevkinite-(Ce) growing along boundaries between alkali feldspar crystals (Afs), Ełk syenite, NE Poland. (**d**) Euhedral chevkinite-(Ce) in pegmatite, Haramosh, Pakistan. (**e**) Acicular perrierite (P), in vug in sanidinite (Sa), Anguillara, Latium, Italy (https://www.e-rocks.com). (**f**) Chevkinite-(Ce) in quartzolite, Rova occurrence, Keivy massif, coexisting with monazite-(Ce) (Mnz), zircon (Zrn), and fergusonite-(Y) (Fer) (Macdonald et al. 2017b). (Color online.)

estimated that GGM groundmass grains in the Little Chief granite porphyry stock, California, crystallized at 700–750 °C and 1.5 kbar, with f_{O_2} >NNO. Liquidus temperatures of between 800 and 900 °C at f_{O_2} close to FMQ were estimated for A-type alkaline granitoid intrusions of the Graciosa Province, Brazil, where CGM are the typical REE phase (Vlach and Gualda 2007). The Paleogene Western Granite on the island of Rum, Scotland, gave the range 808–781 °C at f_{O_2} ~NNO, at P_{H_2O} <1 kbar (Macdonald et al. 2013).

Late magmatic

One form of late magmatic CGM is at grain boundaries between the major phases. Cellai et al. (1993) recorded perrierite-(Ce) up to 30 µm long, generally occurring enclosed in the rims of K-feldspars in an evolved minette from Montecatini Val di Cecina, Tuscany, Italy. Enclosure of CGM within feldspar rims was also noted in weakly peralkaline syenites from the Agua de Pau volcano, São Miguel, Azores Islands, by Ridolfi et al. (2003). Carlier and Lorand (2008) recorded perrierite crystalliz-

ing alongside sanidine and tridymite as late-magmatic phases in kersantites of the Oroscocha volcano; formation conditions were estimated at 950 °C and oxygen fugacity at FMQ+5 log units. The chevkinite-(Ce) shown in Figure 12c grew along boundaries between alkali feldspar crystals in the Ełk syenite, NE Poland. Hezuolinite forms a late magmatic mineral, in association with titanite, loparite-(Ce) and britholite-(Ce)? in lujavrite from Saima (Wu et al. 2016). A further form of late magmatic crystallization is in mesostases and interstices, for example in tholeiitic intrusions (Melluso et al. 2014; Muhling et al. 2014). de Hoog and van Bergen (2000) described perrierite-(Ce) growing in the groundmass of a potassic trachyandesite from the Lewotolo volcano, Indonesia. Chevkinite found as microlites in groundmass glass from high-silica vitrophyres from the Yellowstone caldera, Wyoming, must also represent late magmatic crystallization (Vasquez et al. 2009).

Carbonatites and associated hydrothermal metasomatic rocks

Chevkinite-group minerals are perhaps uncommon components of carbonatite bodies. For example, Berger et al. (2009) recorded chevkinite as occurring in only 4 out of 58 Nb- and REE-bearing carbonatite deposits. Chevkinite-(Ce) was reported in carbonatite of the Bayan Obo Nb-REE-Fe deposit by Shimazaki et al. (2008b) and Smith et al. (2016), associated with tremolite-richterite, barite, monazite-(Ce), bastnäsite-(Ce), fluorbritholite-(Ce), gadolinite-(Ce), FeTi-oxides, and sulfides. Chevkinite also occurs in a sövite dike in the Maoniuping REE deposit, China (Wang et al. 2001; Xu et al. 2008). Shen et al. (2005, p. 216) suggested that the type maoniupingite-(Ce), which occurs in carbonatitic veins and pegmatites at Maoniuping, "directly crystallized from a type of F-, water- and REE-rich mineralizing fluids during the transitional stages of magmatic-hydrothermal processes." Viladkar et al. (2009) reported that chevkinite-(Ce) is the only REE-bearing accessory mineral in carbonatites of the Samchampi massif, suggesting that it formed by hydrothermal alteration of ilmenite or magnetite in the late stages of carbonatite formation. Perrierite-(Ce) occurs concentrated at the endocontact between a carbonatite dike and host melanephelinite in the Danadai alkaline complex, Rajasthan, India (Macdonald et al. 2009). A Nb-rich chevkinite has been found in a carbonate vein in the Biraya Fe-REE deposit by Mills et al. (2012) and Stachowicz et al. (2019 and in review). Makagonov and Muftakhov (2016) reported perrierite-(Ce) in apatite-albite-phlogopite-calcite veins of the the Vishnevogorsky complex, suggesting that they characterized the silicate-to-carbonatite transition in the complex. Sr-Zr-rich perrierite was found in apatite veins in the Mushgai-Khuduk carbonatite complex, Mongolia, by Andreev and Ripp (1995).

The type strontiochevkinite, from a rheomorphic fenite associated with carbonatites at Cerro Sarambi, Paraguay, is estimated by Haggerty and Mariano (1983) to have formed at a depth of ~5 km at high f_{O_2} (much greater than MH) and at T ~500–550 °C.

Albitites occur in several forms, including large concordant bodies, discordant pegmatites and dikes, and albite breccias, and are formed by several mechanisms, such as Na-metasomatism of granitic rocks, partial melting of amphibolites, and liquid immiscibility from gabbroic magma. Proshchenko (1967) reported "chevkinite-(La)" in albitites from eastern Siberia. It would be valuable to restudy this material, to determine whether the La dominance is a function of the paragenesis. Monchoux et al. (2006) recorded chevkinite-(Ce) in igneous albitite dikes intruding lherzolite in the western Pyrenees, France, in association with albite, muscovite, biotite, chlorite, epidote, zircon, titanite, thorite, pyrochlore, aeschynite-(Ce), ferrocolumbite, rutile, ilmenite, magnetite, allanite-(Ce), apatite, and monazite-(Ce). The albitites are thought to have been formed by very low-degree (<1%) partial melting of a shallow mantle, harzburgitic, source previously enriched by carbonate-related metasomatism (Pin et al. 2006).

Pegmatites, quartzolites, and miarolitic cavities

Included in this category are parageneses where a significant fluid phase coexisted with melt.

Pegmatites. Pegmatites are a common host of CGM, with some impressive occurrences (Fig. 12d). Rajesh (2003), for example, noted CGM crystals up to 0.1 m long in pegmatites associated with the Puttetti syenite, India. CGM-bearing pegmatites are generally, but not invariably, associated with syenitic and granitic intrusions, and can be of both metaluminous (Semenov et al. 1966; Mitchell et al. 1976; Miyazaki and Santosh 2005; Prol-Ledesma et al. 2012) and alkaline or peralkaline (Segelstad and Larsen 1978; Čech et al. 1988; Chakhmouradian and Mitchell 1999; Macdonald et al. 2015b) affinity.

Miarolitic cavities. Parodi et al. (1994) described perrierite-Ce) occurring in association with titanite, zircon, and baddeleyite on the walls of miarolitic cavities in an ejected syenite block in the Sabatini complex, Latium, Italy, linking its origin to the late pneumatolitic-pegmatitic stages of the regional volcanic activity (Fig. 12e). Della Ventura et al. (2001) reported perrierite-(Ce) in miarolitic cavities in a syenite block from the Roccamonfina volcano, Latium, which they related to late metasomatic stages. Chevkinite occurs in miarolitic cavities in the Kuiqi peralkaline granite, SE China, associated with *inter alia* apatite, allanite, zircon, titanite, xenotime, and pyrochlore (Martin et al. 1994). The type perrierite-(La) occurs in miarolitic cavities in lava in the Eifel, in association with sanidine, phlogopite, pyrophanite, zirconolite, members of the jacobsite-magnetite series, zircon, and fluorcalciopyrochlore (Chukanov et al. 2012a).

Quartzolites ("silexites" in the Russian literature) are rocks composed primarily of quartz (>60 vol%) and with quartz:feldspar ratios ≥9:1 (Bel'kov et al. 1988; Zozulya and Eby 2010; Macdonald et al. 2017b). They are transitional between higher-temperature orthomagmatic granites and fluid-magmatic rocks, such as pegmatites, and mesothermal hydrothermal rocks. Significant amounts of fluorite and other F- or OH-bearing minerals indicate the active involvement of fluids in their formation. In the Western Keivy massif quartzolites commonly host rare metals, such as the Purnach (Bel'kov and Batieva 1991), Pessarjok (Macdonald et al. 2012) and Rovozero (Macdonald et al. 2012; Lyalina et al. 2014) occurrences. In the Keivy quartzolites, zircon is the main mineral in the ore assemblages, accompanied by various combinations of aeschynite-(Y), chevkinite-(Ce), fergusonite-(Y), britholite-group minerals, yttrialite-(Y), thorite, monazite-(Ce), xenotime-(Y), and bastnäsite-(Ce) (Fig. 12f).

Metamorphic rocks

Chevkinite-group minerals have been recorded in several high-grade metamorphic occurrences (gneisses and associated pegmatites), e.g., Archean charnockitic gneisses in the West Hoggar, Algeria (Acef et al. 2001), from various localities in Antarctica (Atrashenok et al. 1967; Grew and Manton 1979a, 1979b; De Paolo et al. 1982; Harley 1994; Hokada 2007; Belkin et al. 2009; Fig. 13a), and the Eastern Ghats Province, India (Grew and Manton 1986; Belkin et al. 2009; Fig. 13b). Čech et al. (1988) reported chevkinite-(Ce) in a pegmatite associated with a pre-Upper Proterozoic peralkaline quartzo-feldspathic gneiss at Mbolwe Hill, Zambia. CGM-bearing pegmatites are known from the largely granulitic gneiss terrain of the Purulia district, West Bengal, India (Baidya 1992).

Temperatures and pressures of 1000–1180 °C and 3–4 kbar have been estimated for the formation of perrierite in a partially melted sapphirine granulite xenolith from the Vestfold Hills, Antarctica (Harley 1994; Harley and Christy 1995), and temperatures up to 1100 °C in granulites of the Archean Napier Complex, Antarctica (Harley 2008). The high Al content of the perrierite (≤9 wt%; Supplemental[1] Table S3b) has been attributed to the high pressures of crystallization. This is consistent with experimental evidence; in CGM crystallized from a series of REE-enriched compositions ranging from basalt through andesite to rhyolite at pressures from 7.5 to 20 kbar and temperatures from 900–1050 °C, the Al content of the CGM increased with increasing pressure (Green and Pearson 1988) (Fig. 10).

The type examples of the rare minerals, rengeite and matsubaraite (Fig. 13c), occur in jadeitite in the high *P-T* type Renge belt, Itoigawa-Ohmi-district, Japan (Miyajima et al. 2001, 2002). The belt (330–280 Ma) was metamorphosed under glaucophane-schist to epidote-amphibolite facies conditions. Chevkinite-(Ce) and perrierite-(La) occur in different layers of Proterozoic metacarbonate rocks at Golden Lake, Ontario (Macdonald et al. 2009) (Fig. 13d). No study has yet examined the factors stabilizing the different phases.

So far as we know, CGM have not yet been recorded in a low-grade metamorphic rock although, given their occurrence in hydrothermal and ore deposits, such parageneses cannot be precluded. Neither has a CGM been reported growing in a low-temperature sedimentary environment.

A potentially rewarding study would be the role of CGM in influencing REE and HFSE behavior during partial melting of crustal rocks. Hokada (2007), for example, suggested that the conditions for the formation of perrierite in an ultrahigh-temperature (UHT) sapphirine-quartz gneiss from East Antarctica might have been achieved by the generation of an anatectic melt, leaving the LREE and Ti, incorporated into the perrierite,

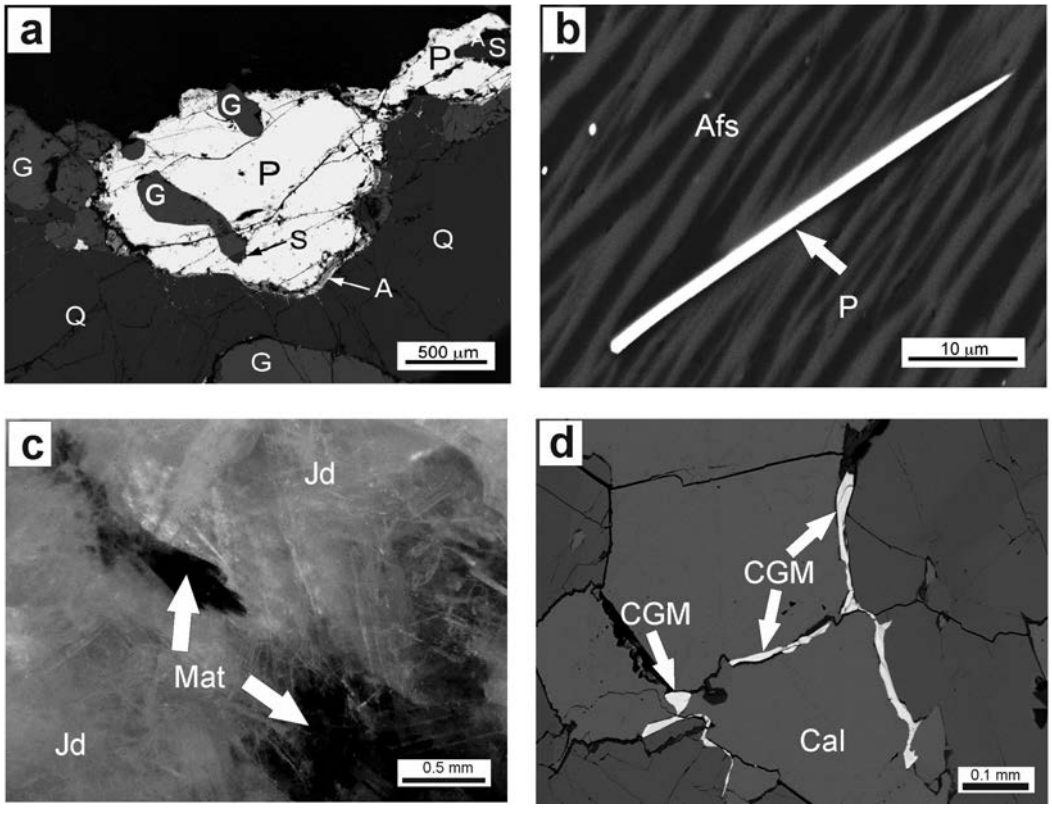

Figure 13. BSE images of CGM in metamorphic rocks. (**a**) Perrierite (P) with inclusions of garnet (G) and sillimanite (S) in a quartz and garnet assemblage, quartzofeldspathic granulite from the Napier Complex, East Antarctica (from Belkin et al. 2009). (**b**) Acicular perrierite in mesoperthite, in migmatitic sapphirine granulite, Anakpalle, south India (from Belkin et al. 2009). (**c**) Matsubaraite (Mat) in jadeitite (Jd), Itoigawa-Ohmi district, Niigata prefecture, Japan (from Miyajima et al. 2002). (**d**) CGM (Chv) along with contact between carbonate crystals, metacarbonate, Golden Lake, Ontario.

behind in the solid rock. Another natural laboratory for such studies might be a migmatite suite where the products of partial melting and their subsequent evolution can be recognized. For example, Johnson et al. (2003) have inferred a genetic connection between migmatites, leucosomes, dikes, and peraluminous granites in the Proterozoic Dalradian rocks of NE Scotland, but no study has been made of the accessory minerals from this rock suite, and how their assemblages and compositions varied as the inferred melting proceeded.

Skarns

Chevkinite-group minerals occur in calc-skarns of eastern Tuva and eastern Siberia, where they formed in fissures in association with pyrochlore, fergusonite, fluorite, phenakite, meliphanite, and zircon (Kudrin et al. 1967). Ontoyev (1993) described, from the Bayan Obo rare-earth deposit, CGM in humite and humite-clinohumite skarns formed at or close to the contacts between dolomites and syenitic rocks. Associated minerals are humite, clinohumite, spinel, periclase, phlogopite, allanite, fluorite, and titanomagnetite. The skarns are thought to have formed at temperatures >500 °C. The type dingdaohengite-(Ce) was first recognized in magnesian skarns at Bayan Obo (Xu et al. 2008).

Chevkinite-group minerals can also form by recrystallization of primary CGM by interaction with metasomatic fluids. For example,Macdonald et al. (2015d) described, in a quartz-epidote metasomatite from the Khaldzan Buregtey massif, Mongolian Altai, prismatic chevkinite-(Ce) crystals up to 8 × 1.5 cm in size that had grown by recrystallization and enlargement of the same mineral in the precursor pegmatite where it never exceeded 1 mm in size.

The range of occurrences testifies to the ability of CGM to form under very diverse, relatively low temperature conditions, with different fluid compositions, and in a multitude of parageneses. Quantifying the variables active during their formation will undoubtedly be difficult: REE-bearing deposits can be formed in several stages, with changes in temperature and fluid composition(s) and under disequilibrium conditions.

Hydrothermal alteration of CGM

The presence of even moderate concentrations of actinides makes the CGM prone to metamictization (e.g., <0.5 wt% ThO_2; Sokolova et al. 2004). The structural damage, in turn, promotes entry of water into the structure; thus in common with other accessory minerals, such as apatite, monazite, and xenotime, CGM can be susceptible to alteration by magmatic and/or hydrothermal fluids. Studies of the hydrothermal alteration of CGM go back at least as far as that of Lacroix (1915) and were then pursued chiefly by Russian workers, such as Mineev et al. (1962), Marchenko et al. (1968), and Rozanov et al. (1983). We discuss here only more recent work where microanalytical techniques have allowed a more complete characterization of the phases involved in the alteration.

Three general replacement schemes can be recognized: (1) compositional modification of the CGM produced a zone of "altered chevkinite" (Jiang 2006; Vlach and Gualda 2007; Bagiński et al. 2015); (2) formation of this zone was followed by the development of a new mineral assemblage (Jiang 2006; Macdonald et al. 2015b, 2015c); and (3) alteration proceeded directly to the formation of a new assemblage (Macdonald et al. 2015d; Bagiński et al. 2016). The examples provided below were chosen to describe the three schemes and to show the effects of different ligands on the alteration products.

"Altered chevkinite"

Bagiński et al. (2015) described the alteration of chevkinite-(Ce) in quartzolite from the Keivy massif, where the mineral was replaced by a presumably amorphous phase that, lacking structural information, they simply termed altered chevkinite, after the usage by Jiang (2006) and Vlach and Gualda (2007). In places, the altered material is present as rims on the unaltered CGM, or developed along fractures (Fig. 14a). Elsewhere, the alteration proceeded to a very complex mixture of unidentified phases of different BSE brightness, occurring as amoeboid patches and fibers (Bagiński et al. 2015). No structural data exist for these phases. The compositional modification of the CGM during alteration is described below.

Alteration of CGM with formation of new phases

In some cases, the formation of altered chevkinite was followed by the formation of a different phase assemblage. This progression presumably reflected the continuity of fluid input and the aggressivity of the fluid (essentially its temperature and content of ligands).

In a study of hydrothermally altered chevkinite-(Ce) in syenites of the Shuiquangou intrusion, China, Jiang (2006) found that the chevkinite was replaced by an allanite-ilmenite association in the inner part of a corona texture, either directly or via a thin zone of altered chevkinite. This was in turn mantled by a ring of allanite, titanite, and ilmenite and then by a distal rim of epidote. A detailed description of element redistribution during replacement was given. Jiang (2006) did not specify the composition of the fluid, but from the nature of the alteration assemblage it apparently had low F and CO_2 contents. Hydrothermal alteration of CGM to allanite and titanite was also recorded by Savel'eva and Karmanov (2008, 2010), Hirtopanu et al. (2013) and Papoutsa and Pe-Piper (2013).

A broadly similar replacement sequence to that in Jiang (2006) was reported by Macdonald et al. (2015c) in chevkinite-(Ce) from a quartz-epidote metasomatite from the Keivy massif. In this case, the allanite zone comprises ferriallanite-(Ce) and davidite-(La), rimmed by a zone of allanite-(Ce) richer than the ferriallanite-(Ce) in the epidote component, and there is no ilmenite in the titanite-rutile mantle (Fig. 14b). Rare-earth carbonates, aeschynite-(Ce) and aeschynite-(Y) were accessory minerals in all the alteration zones. The hydrothermal fluids were inferred to have had high Ca activities and significant contents of F and CO_2. Li and Zhou (2017) have also recorded replacement of chevkinite-(Ce) by allanite-(Ce) and aeschynite-(Ce) from the Sin Quyen deposit.

A complex alteration sequence was described in a syenitic pegmatite from the Vishnevye Mountains by Macdonald et al. (2015b). The chevkinite-(Ce) was altered, via a series of texturally complex intermediate steps, to a bastnäsite-(Ce)-ilmenite-columbite-(Fe) assemblage (Fig. 14c). The intermediate stages involved partial replacement and formation of symplectite texture. An approach to equilibrium was achieved only during the

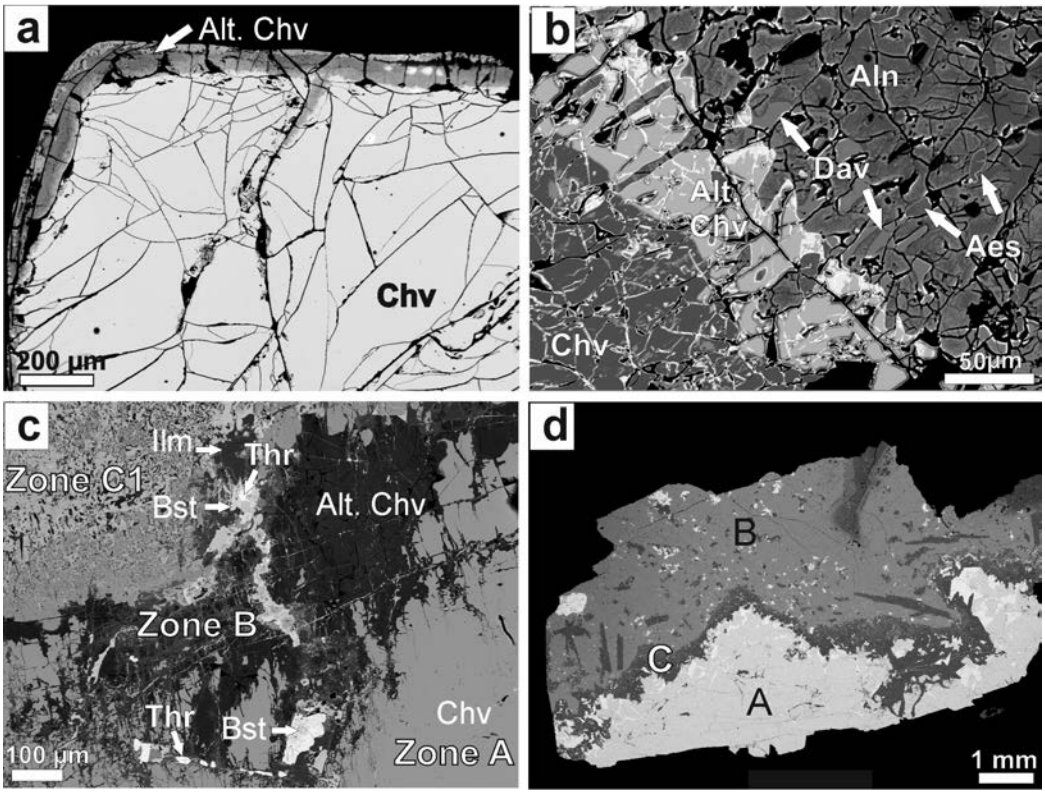

Figure 14. BSE images of various examples of CGM alteration. (**a**) Chevkinite-(Ce) (Chv) crystal altered along its rim and along internal cracks (Alt. Chv), in quartzolite, Keivy massif (from Bagiński et al. 2015). (**b**) Chevkinite-(Ce) partially replaced by ferriallanite-allanite-(Ce) (Aln), davidite (Dav), and aeschynite (Aes); in metasomatite, Keivy massif, Kola massif (from Macdonald et al. 2015c). (**c**) Chevkinite-(Ce) (Zone A) replaced first by altered chevkinite (Zone B) and then by a bastnäsite–ilmenite–thorite (Bst–Ilm–Thr) assemblage (C1), veins of which have penetrated into the chevkinite; metasomatite, Keivy massif, Kola Peninsula (from Macdonald et al. 2015b). (**d**) Chevkinite-(Ce) (A) replaced first by minerals of the epidote supergroup (B) and then by titanite-rutile-cerite-REE carbonate assemblages (C). From Macdonald et al. (2015d).

final stages of alteration. The hydrothermal fluids were inferred to have been F- and CO_2-rich, with variable levels of Ca activity.

Ignoring the complexities of the intermediate stages, the *critical* reaction in the alteration of the chevkinite-(Ce) was given as:

$$2[Ce_{3.5}Ca_{0.5})_{\Sigma 4}Fe(Fe_{1.5}Ti_{0.5})_{\Sigma 2}Ti_2(Si_2O_7)_2O_8] + 8CO_2 + 7F^- =$$
chevkinite-(Ce)
$$7CeCO_3F + 5FeTiO_3 + 8SiO_2 + CaCO_3 + 5O^{2-}$$
bastnäsite ilmenite quartz

Li and Zhou (2017) described replacement of chevkinite-(Ce) by allanite-(Ce) + aeschynite-(Ce) ± bastnäsite-(Ce) ± columbite-(Fe) ± ilmenite at Sin Quyen.

Alteration directly to new phases

A quartz-epidote metasomatite from the Khaldzan Buregtey massif is an example of alteration of a CGM proceeding directly to new phases (Fig. 14d) (Macdonald et al. 2015d). A peralkaline granite pegmatite was metasomatized by hydrothermal fluids, where minerals in the pegmatite, including chevkinite-(Ce), fergusonite-(Y) and epidote supergroup minerals, were recrystallized and texturally coarsened at temperatures in the range 318–446 °C. An influx of low-temperature fluids (156–160 °C) resulted, *inter alia*, in the replacement of chevkinite-(Ce) by titanite-cerite-(Ce)-REE carbonate assemblages. The hydrous fluids were interpreted to have been acidic and oxidizing, with significant amounts of CO_2 but poor in F and Cl.

Many other replacement schemes undoubtedly exist. Kartashov (1994; reaction 3), for example, proposed a reaction involving high Ca and CO_2 activities for altered chevkinite from the Khaldzan Buregtey massif:

$$Ce_4Fe(Fe,Ti)_2Ti_2Si_4O_{22} + Fe^{2+} + 4Ca^{2+} + 8CO_3^{2-} + 2H_2O \rightarrow$$
chevkinite REE
$$4CaCe(CO_3)_2(OH) + 3FeTiO_3 + 4SiO_2$$
carbonate ilmenite quartz

As further examples, Mitchell et al. (1976) described perrierite with alteration crusts of halloysite, monazite, and anatase in a granitic pegmatite from Bedford County, Virginia, and Prol-Ledemsa et al. (2012) reported replacement of perrierite-(Ce) by a symplectitic intergrowth of allanite-(Ce) + titanite + thorite in the El Muerto granitic pegmatite. Vasyukova and Williams-Jones (2016) reported, in an inclusion in granite from the Strange Lake pluton, chevkinite-(Ce) being locally replaced by karnasurtite-(Ce) $[(Ce,La,Th)(Ti,Nb)(Al,Fe^{3+})(Si,P)_2O_7(OH)_4 \cdot 3H_2O]$ or, in some cases, by an intergrowth of bastnäsite-(Ce), fluorite,

and a Na-deficient variety of gagarinite-(Y) [$Na(REE_xCa_{1-x})(REE_yCa_{1-y})F_6$].

Important studies remain to be made of the controls of the different replacement sequences

In considering the difference between columbite-bearing and columbite-free sequences, Macdonald et al. (2015b) suggested that columbite has low solubility in CO_2-rich fluids, resulting in two potential assemblages: (1) ilmenite + titanite + rutile + (Nb,REE)-oxides = low $X(CO_2)$ and higher Ca or (2) ilmenite + columbite + REE-carbonate = high $X(CO_2)$ and lower Ca.

The examples above show that the alteration products of CGM are dependent on the compositions of the host rock and CGM, the pressure and temperature and the composition of the fluids, in particular, the activities of Ca, F, and CO_2. Studies of the fluids are, however, hampered by their loss from the system and by the fact that they may change composition as alteration proceeds. In the case of the CGM, difficulties in interpreting the record of the passage of fluids through the rocks are exacerbated by the lack of any experimental information on CGM-fluid interactions, in contrast, for example, to monazite (Harlov and Hetherington 2010; Budzyń et al. 2011; Harlov et al. 2011; Harlov 2015).

Compositional modifications during hydrothermal alteration to altered chevkinite

Bagiński et al. (2015) outlined some of the compositional changes occurring in CGM during interaction with hydrothermal fluids. Initial alteration generally results in Ca enrichment, but with increasing degrees of alteration, Ca abundances fall, as do those of the REE, Fe, and Si. Levels of Ti increase strongly, with less marked enrichment in Nb ± Th. Oxide totals of the altered phase are very low (sometimes <90 wt%) and cation totals are not stoichiometric. As a measure of the degree of alteration, the parameter Ti* was introduced by Bagiński et al. (2015), defined as (total Ti apfu – 2), i.e., a measure of the Ti excess over that filling the D site. Figure 15 shows the variation of Ti* and Ca in CGM from various suites. The data generally follow a looped distribution, somewhat arbitrarily divided in the inset into unaltered, partly altered and strongly altered segments.

The overall compositional variations during alteration in many ways mirror in the initial stages those produced by magmatic crystallization and, as in that process, the trend may cross the empirical boundary between the chevkinite and perrierite subgroups, but this time from chevkinite to perrierite (Vlach and Gualda 2007) (Fig. 16). For comparison, perrierite from apatite-albite-phlogopite-calcite veins in the Vishnevogorsky complex also became more calcic with increasing hydration (Makagonov and Muftakhov 2016). Are there ways of telling whether compositional zonation in a given CGM results from hydrothermal alteration rather than crystallization? Using A-type syenites and granites of the Graciosa Province, Brazil, Vlach and Gualda (2007) noted that magmatic chevkinites followed (quasi-) horizontal trends on a Th-Ti plot, whereas altered CGM followed positive trends. Furthermore, as noted above progressive alteration is almost always accompanied by a decrease in oxide totals and increasingly non-stoichiometric structural formulas.

Payette and Martin (1988) gave a description of the alteration of chevkinite-(Ce) in alkali granites of the Welsford igneous complex, New Brunswick, Canada. They reported altered "chevkinite" with remarkable levels of Ti enrichment (up to 7.17 apfu; 50.6 wt% TiO_2). Compared to other altered occurrences, the chevkinite shows strong Ca depletion starting from Ti* values of 1 (Fig. 15). This occurrence would undoubtedly repay

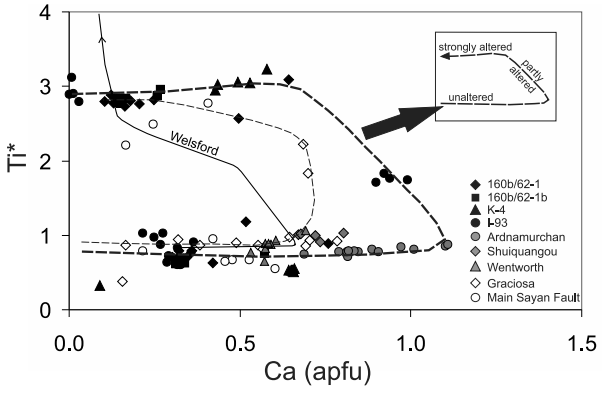

Figure 15. Ca plotted against Ti* (total Ti–2 apfu) for various suites carrying altered CGM. Data sources: samples numbered 160b are from the El'ozero occurrence, Keivy (Bagiński et al. 2015); K4 = syenitic pegmatite, Vishnevye Mountains (Macdonald et al. 2015b); 1–93 = quartzolite, Rova occurrence, Keivy (Macdonald et al. 2012; Bagiński et al. 2015); Ardnamurchan = Paleogene granite, Scotland (Macdonald et al. 2013); Shuiquangou syenite, China (Jiang 2006); Wentworth granite, Nova Scotia (Papoutsa and Pe-Piper 2013); Main Sayan Fault, southern Baikal, Russia (Savel'eva and Karmanov (2008). The inset shows a generalized trend from unaltered to strongly altered phases, based on the solid dashed trend in the main figure. The thin dashed line is for the Graciosa Province (Vlach and Gualda 2007). From Bagiński et al. (2015), except the Welsford trend, drawn from data for sample AGP-1 in Payette and Martin (1988).

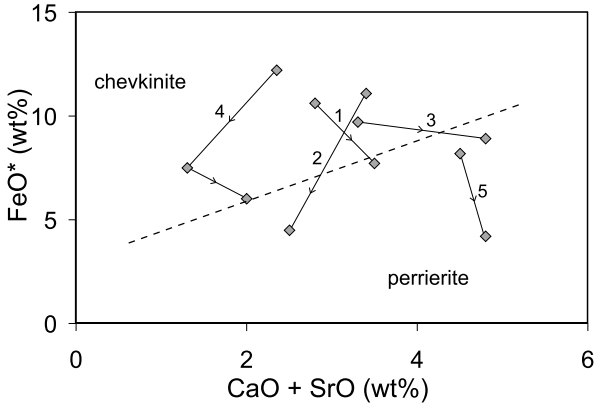

Figure 16. (CaO+SrO) – FeO* plot to show how hydrothermal alteration can drive CGM across the empirical boundary between the chevkinite and perrierite subgroups (Macdonald et al. 2009). The trends are opposite to those formed by magmatic crystallization (Fig. 5). 1 = A-type syenites and granites, Corupá, Brazil (Vlach and Gualda 2007); 2 = syenitic pegmatite, Vishnevye Mountains (Macdonald et al. 2015b); 3 = Shuiquangou syenite (Jiang 2006); 4 = quartzolite, Rova occurrence, West Keivy massif (Bagiński et al. 2015); 5 = carbonate veins, Vishnevogorsky complex (Makagonov and Muftakhov 2016).

a detailed study of the structural, textural, and compositional changes during the alteration process(es).

Implications

Geochemical modeling

Chevknite-group minerals (CGM) occurring as phenocrysts or as inclusions in early crystallized minerals in plutonic rocks may strongly influence trace element distribution during fractional crystallization of intermediate to felsic magmas. In several igneous rock suites, for example, CGM have been the dominant control over LREE distribution (Vlach and Gualda 2007; Hokada 2007; Viladkar et al. 2009; Macdonald et al. 2013; Padilla and Gualda 2016). As an indication of its fractionation potential, Troll et al. (2003) calculated that crystallization of 0.05 wt% chevkinite from a peralkaline rhyolite (comendite) magma with 300 ppm Ce would produce 207 ppm in the residual melt. The CGM may also play an important role in controlling trace element behavior during partial melting of crustal rocks; where refractory, they could retain such elements in the restite (Green and Pearson 1988; Hokada 2007).

Testing of geochemical models requires a detailed knowledge of the partitioning of trace elements between CGM and host melts. The most complete information on the partitioning of REE between CGM and coexisting melts comes from high-silica rhyolites, including comendites from the Olkaria complex, Kenya (Macdonald et al. 2002; Marshall et al. 2009), Gran Canaria (Troll et al. 2003), and from the metaluminous Peach Spring Tuff (Padilla and Gualda 2016). All three data sets show strong partitioning of the LREE into chevkinite-(Ce), with apparent partition coefficients for La and Ce exceeding 1000 (Supplemental[1] Table S5). Chevkinite-(Ce) also concentrates the HREE, although less strongly. In all cases, Ce/Ce* values in chevkinite-(Ce) microphenocrysts are closely similar to those in matrix glass, indicating that CGM crystallization does not significantly affect the size of the Ce anomaly. Similarly, Eu anomalies are fairly comparable in CGM and coexisting glasses and are not affected by CGM crystallization. There is a similar situation in the metaluminous Peach Springs Tuff rhyolite.

Although the partition coefficients are for chevkinite-(Ce) in a compositionally similar set of rocks (high-silica rhyolites), there are some important inter-rock differences. For example, two samples have steep decreases at Eu, two do not (Fig. 17). The apparent partition coefficient for Sr in the Gran Canaria chevkinite-(Ce) (84) greatly exceeds those in Olkaria (≤27). Such differences may be related in part to the crystallization of other accessory minerals, such as allanite or titanite. In their study of chevkinite-(Ce) and titanite microphenocrysts in a Gran Canaria ignimbrite, for example, Troll et al. (2003) found that (1) the chevkinite-(Ce) was enriched in LREE by some three orders of magnitude above that of the glass matrix, whereas titanite was enriched by only 1.5 orders of magnitude; (2) the titanite, but not the chevkinite-(Ce), showed minima at La and Eu on chondrite-normalized REE plots; and (3) the titanite was more sensitive to melt composition than the chevkinite-(Ce). They concluded that chevkinite, where present, might be the controlling REE-bearing phase in peralkaline rhyolitic magmas. Padilla and Gualda (2016) found, in the metaluminous Peach Spring Tuff, that whereas chevkinite-(Ce) concentrated the LREE more efficiently than other minerals, titanite had a significant preference for the REE between Sm and Ho.

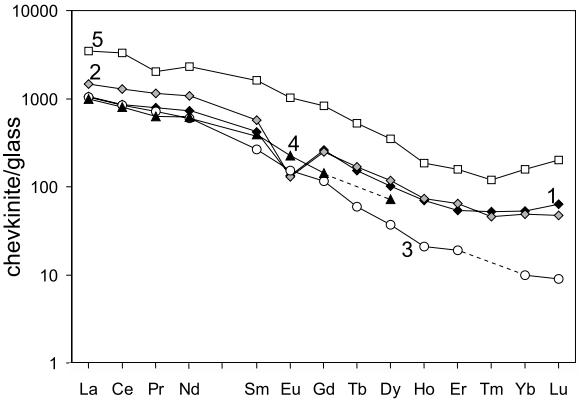

Figure 17. Apparent chevkinite/melt partition coefficients for REE in mildly peralkaline (1 to 4) and metaluminous (5) rhyolites. 1 = ignimbrite X, Gran Canaria (Troll et al. 2003); 2 and 4 = samples SMN49 and ND002, Olkaria complex, Kenya Rift Valley (Macdonald et al. 2002); 3 = sample BL210b, Olkaria (Marshall et al. 2009); 5 = Peach Springs Tuff, Arizona (Padilla and Gualda 2016).

These studies have clearly shown that, to be most valuable, partition coefficients should be determined for individual suites and that any accessory cannot be treated in isolation from any coexisting phases. A potentially rewarding way forward is via a detailed examination of multi-phase accessory assemblages in volcanic rocks (Padilla and Gualda 2016). For example, many Cenozoic latite to rhyolite eruptive sequences of Nevada, U.S.A., have microphenocryst assemblages containing various proportions of titanite, allanite, perrierite, apatite, zircon, and monazite (Broxton et al. 1989; Warren et al. 1989). In the example shown in Figure 18, from the Devine Canyon Tuff, Oregon, four accessory phases (CGM, REE-Si-bearing apatite, zircon, and ilmenite) were incorporated into a growing clinopyroxene, with the enclosing glass acting as a guide to the melt composition. By documenting specific textural relationships, such assemblages provide an excellent opportunity to distinguish the effects of melt composition, temperature, and f_{O_2} on mineral stabilities and to track the partitioning of elements into the accessory phases.

The relationships between CGM and other REE-bearing accessory phases

It is important to understand as fully as possible the relationships between the CGM and other accessory minerals coexisting in the same rocks. During equilibrium or near-equilibrium crystallization, the first major REE phase to appear may preclude or have a tendency to limit the abundance of the other competing phase(s). Such relationships will determine *inter alia* trace element fractionation paths in residual melts and our ability to decipher *P-T-*f_{O_2} conditions during magma crystallization. Determining the stability relationships between CGM and coexisting accessory minerals may, however, be extremely difficult due to the textural complexities and ambiguities and to the non-equilibrium conditions under which the minerals often form. In this section, some aspects of the relationships between CGM and two REE-bearing phases, allanite and monazite, in igneous suites are described.

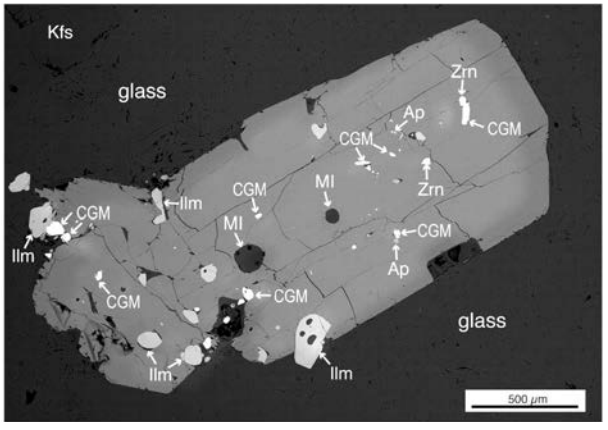

Figure 18. Slightly reversely zoned hedenbergite from the Devine Canyon Tuff, Juntura, Oregon, U.S.A., sample DCT_B. The crystal is filled with silicate melt inclusions (MI) and various solid inclusions, such as ilmenite (Ilm), REE-Si-rich apatite (Ap), zircon (Zrn), and chevkinite-(Ce) (CGM). The hedenbergite is surrounded by glass (Gl), with phenocrysts of alkali feldspar.

Reconnaissance experiments by Vasquez et al. (2004) showed that allanite saturation in high-silica rhyolites occurred at 760–770 °C, whereas at 780 °C, chevkinite replaced allanite. This is consistent with textural evidence of allanite mantling chevkinite in granites from the Aztec Wash Pluton, Nevada (Robinson and Miller 1999), Paleogene granites (Macdonald et al. 2013), and the Lucerne intrusion, Maine, U.S.A. (Fig. 19a) (Prol-Ledemsa et al. 2012) have reported perrierite-(Ce) inclusions up to 5 cm across occurring in allanite in the wall zone and first intermediate zone of the El Muerto granitic pegmatite. Vlach and Gualda (2007) showed that in the A-type granites of the Graciosa Province, Brazil, chevkinite-(Ce) is the main REE phase in metaluminous syenites, alkali-feldspar syenites and peralkaline alkali-feldspar granites of the alkaline association, while allanite-(Ce) is the main REE phase in the aluminous association.

In cooling silicate liquids, monazite is the only common accessory phase with a REE abundance similar to CGM. Monazite solubility increases with increasing peralkalinity (Montel 1986, 1993) and decreases with increasing alumina saturation index (Rapp et al. 1987). In contrast, we know of no record of a CGM in a peraluminous granite. This may suggest that CGM are favored in metaluminous and peralkaline melts vs. peraluminous melts.

Monazite and CGM do seem to be able to coexist, apparently in, or close to, equilibrium. Hokada (2007) recorded perrierite and monazite in sapphirine-quartz gneiss from the Napier Complex, East Antarctica, noting that the perrierite is the dominant phase. Monazite and CGM coexist in the Boso and Noto volcanics (Miyawaki et al. 2012). Liu et al. (2015) reported subhedral monazite-(Ce) and chevkinite in a lithic clast in a martian breccia meteorite. In a quartzolite from the Rova occurrence, Keivy massif, Macdonald et al. (2017b) found that chevkinite-(Ce) and monazite-(Ce) formed part of the primary crystallizing as-

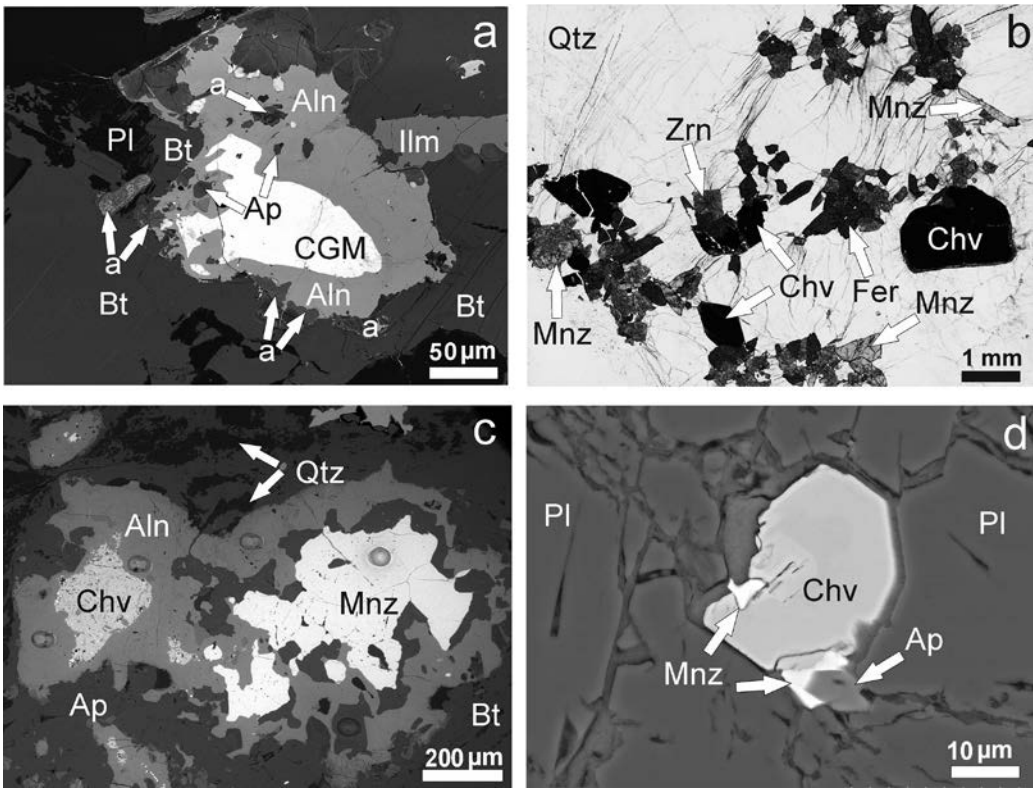

Figure 19. (**a**) A chevkinite-(Ce) (CGM) crystal that has partially reacted to form allanite-(Ce) (Aln), Lucerne Granite, Hancock County, Maine, U.S.A. Later alteration, marked "a", around the periphery of the allanite-(Ce) has removed most of the REE. Note the bottom middle two arrows indicating a scalloped reaction front. Other phases are biotite (Bt), apatite (Ap), ilmenite (Ilm), and plagioclase (Pl). (**b**) Chevkinite-(Ce) and monazite-(Ce) apparently growing in equilibrium, in association with zircon and fergusonite-(Y), in quartzolite, Keivy massif (from Macdonald et al. 2017b). (**c**) Chevkinite (Chv) and monazite (Mnz) mantled by allanite, Sin Quyen (Li and Zhou 2017). An irregular layer of fluorapatite (Ap) lies between the monazite and allanite. Image courtesy of X.-C. Li. (**d**) Chevkinite-(Ce) (Chv) in plagioclase, with late monazite-(Ce) (Mnz) on rims. Cañada Pinabete granite, Questa complex, New Mexico.

semblage, in association with fergusonite-(Y) and zircon (Fig. 19b). Li and Zhou (2017, 2018) reported that monazite-(Ce) and chevkinite-(Ce) formed together from high-temperature fluids, and were subsequently mantled by allanite (Fig. 19c), in the early ore-forming stage at Sin Quyen. Monazite crystallization post-dating that of CGM is recorded in a perrierite-(Ce) in plagioclase, with late monazite-(Ce) on the CGM rims, Cañada Pinabete granite, Questa complex, New Mexico (Fig. 19d).

Thus, while it appears that the relationship between CGM and allanite is generally determined by melt composition and temperature, that between CGM and monazite is more complex, especially in the low-temperature regime where fluid composition and availability become important factors.

Geochronology

Several studies have demonstrated the usefulness of CGM in geochronology in rocks ranging from Archean to Recent. Using U-Th-Pb elemental ratios, Hokada (2007) found a chemical age of 2460 ± 110 Ma for perrierite from a sapphirine gneiss of the Napier Complex. In situ sensitive high-resolution ion microprobe (SHRIMP) U-Pb methods were employed by Rasmussen et al. (2014) to date CGM from a tholeiitic sill of the Eel Creek Formation, Western Australia (~1.07 Ga), but high common Pb contents resulted in an unreliable date. Min et al. (2006) used the (U-Th)/He method to date (1.62 ± 0.11 Ma) volcanic phenocrysts with chevkinite and britholite inclusions, in the Jemez Volcanic Field, New Mexico. Vasquez et al. (2014) reported ^{238}U-^{230}Th dating of chevkinite in rhyolites from La Primavera, Mexico (125–85 ka) and Yellowstone (110–250 ka) calderas. A potentially useful project would be to use CGM altered by interaction with hydrothermal fluids to date the alteration event but, so far as we know, no such study has yet been published.

CGM and magma mixing

Given the ubiquity of magma mixing in the evolution of igneous suites, an interesting question is whether the CGM have been used to identify the process. The accessory mineral assemblage titanite, perrierite, zirconolite, and baddeleyite was reported as late magmatic phases in kersantites of the Oroscocha volcano by Carlier and Lorand (2008). The assemblage formed under low water pressure and high f_{O_2} (FMQ+5), the strongly oxidizing conditions having been promoted by magma mixing between lamprophyric and felsic end-members. Macdonald et al. (2013) ascribed reverse zoning and resorbed textures in chevkinite-(Ce) to possible magma mixing in A-type granites of the U.K. Paleogene province but did not present robust evidence as to the nature of the mixing components.

Acknowledgments

We thank Fernando Camara, Pavel Kartashov, Silvio Vlach, Mark Welch, and Dmitry Zozulya for educating us in many aspects of CGM: we gratefully acknowledge their insights and expertise. Anton Chakhmouradian and Janet Muhling provided very detailed and helpful reviews of the manuscript. We also thank Dan Harlov for editorial handling and him and Keith Putirka for encouraging us to prepare this review.

References cited

Acef, K., Ouzegane, K., and Kienast, J.R. (2001) Archean alkaline charnockitic gneisses in the In Ouzzal granulitic unit, West Hoggar, Algeria. Special Abstract Issue, EUG XI. Strasbourg, France, 571.

Andreev, G.V., and Ripp, G.S. (1995) About perrierite found in apatite ore. Proceedings of the Russian Mineralogical Society, 124, 83–84 (in Russian).

Atrashenok, L.Ya., Avdzeyko, G.V., Klimov, A.V., Krylov, A.Ya., and Silin, Yu.I. (1967) Comparative data on absolute ages of Antarctic rocks (lead and argon methods). In Questions of the Dating of the Most Ancient (Katarchean) Geological Formations and of Basic Rocks, p. 227–229. Izdatelstvo Nauka, Moscow (in Russian).

Azambre, B., Rossy, M., and Lago, M. (1987) Caractéristiques pétrologiques des dolérites tholéiitiques d'âge triasique (ophites) du domaine pyrénéen. Bulletin de Minéralogie, 110, 379–396.

Bagiński, B., and Macdonald, R. (2013) The chevkinite group: underestimated accessory phases from a wide range of parageneses. Mineralogia, 44 (2-3). DOI: 10.2478/mipo-2013-0006.

Bagiński, B., Macdonald, R., Dzierżanowski, P., Zozulya, D., and Kartashov, P.M. (2015) Hydrothermal alteration of chevkinite-group minerals: products and mechanisms. Part 1. Hydration of chevkinite-(Ce). Mineralogical Magazine, 79, 1019–1037.

Bagiński, B., Zozulya, D., Macdonald, R., Kartashov, P.M., and Dzierżanowski, P. (2016) Low-temperature hydrothermal alteration of a rare-metal rich quartz-epidote metasomatite from the El'ozero deposit, Kola Peninsula, Russia. European Journal of Mineralogy, 28, 789–810.

Baidya, T.K. (1992) A note on some uranium-thorium bearing pegmatoids of Nawahatu area, Purulia district, West Bengal. Indian Minerals, 46, 175–176.

Belkin, H.E., Macdonald, R., and Grew, E.S. (2009) Chevkinite-group minerals from granulite-facies metamorphic rocks and associated pegmatites of East Antarctica and South India. Mineralogical Magazine, 73, 149–164.

Bel'kov, I.V., and Batieva, I.D. (1991) New data on rare-metal mineralogy of silexites stock within the Purnach alkali granite pluton. In New Data on Mineralogy of Rare Elements in Kola Peninsula, p. 15–19 (in Russian). Apatity: Kola Science Center, USSR Academy of Sciences,.

Bel'kov, I.V., Batieva, I.D., Vinogradova, G.V., and Vinogradov, A.N. (1988) Mineralization and fluid regime in the contact zones of alkali granite intrusions. Kola Branch, USSR, Academy of Sciences, Apatity, pp. 110 (in Russian).

Berger, V.I., Singer, D.A., and Orris, G.J. (2009) Carbonatites of the world, explored deposits of Nb and REE—database and grade and tonnage models. U.S. Geological Survey Open-File Report 2009-1139, 17 pp.

Bindeman, I.N., and Valley, J.W. (2003) Rapid generation of both high- and low-$\delta^{18}O$, large-volume silicic magmas at the Timber Mountain/Oasis Valley caldera complex, Nevada. Geological Society of America Bulletin, 115, 581–595.

Broxton, D.E., Warren, R.G., Byers, F.M., and Scott, R.B. (1989) Chemical and mineralogical trends within the Timber Mountain-Oasis Valley caldera complex, Nevada: evidence for multiple cycles of chemical evolution in a long-lived silicic magma system. Journal of Geophysical Research, 94, 5961–5985.

Budding, K.E., Cunningham, C.G., Zielinski, R.A., Steven, T.A., and Stern, C.R. (1987) Petrology and chemistry of the Joe Lott Tuff Member of the Mount Belknap volcanics, Marysvale volcanic field, west-central Utah. U.S. Geological Survey Professional Paper, 1354, 47 pp.

Budzyń, B., Harlov, D.E., Williams, M.L., and Jercinovic, M.J. (2011) Experimental determination of stability relations between monazite, fluorapatite, allanite, and REE-epidote as a function of pressure, temperature, and fluid composition. American Mineralogist, 96, 1547–1567.

Calvo, C., and Faggiani, R. (1974) A re-investigation of the crystal structures of chevkinite and perrierite. American Mineralogist, 59, 1277–1285.

Cameron, K.L., and Cameron, M. (1986) Whole-rock/groundmass differentiation trends of rare earth elements in high-silica rhyolites. Geochimica et Cosmochimica Acta, 50, 759–769.

Carlier, G., and Lorand, J.-P. (2008) Zr-rich accessory minerals (titanite, perrierite, zirconolite, baddeleyite) record strong oxidation associated with magma mixing in the south Peruvian potassic province. Lithos, 104, 54–70.

Čech, F., Povondra, P., and Vrána, S. (1988) Crystal chemistry of chevkinite from Zambia. Acta Universitatis Carolinae: Geologica, no. 2, 181–193.

Cellai, D., Conticelli, S., and Diella, V. (1993) Perrierite-chevkinite in igneous ultrapotassic rocks from Central Italy: chemical data and their petrological significance. Periodico di Mineralogia, 62, 57–66.

Chakhmouradian, A.R., and Mitchell, R.H. (1999) Primary, agpaitic and deuteric stages in the evolution of accessory Sr, REE, Ba and Nb-mineralization in nepheline-syenite pegmatites at Pegmatite Peak, Bearpaw Mountains, Montana. Mineralogy and Petrology, 67, 85–110.

Chukanov, N.V., Blass, G., Pekov, I.V., Belakovskiy, D.I., Van, K.V., Rastsvetaeva, R.K., and Aksenov, S.M. (2012a) Perrierite-(La), $(La,Ce,Ca)_4(Fe^{2+},Mn)(Ti,Fe^{3+},Al)_4(Si_2O_7)_2O_8$, a new mineral species from the Eifel volcanic district, Germany. Geology of Ore Deposits, 54, 647–655.

Chukanov, N.V., Aksenov, S.M., Rastsvelaeva, R.K., Belakovskiy, D.I., Göttlicher, J., Britvin, S.N., and Möckel, S. (2012b) Christofschäferite-(Ce), $(Ce.La_4Ca)_4Mn^{2+}(Ti,Fe^{3+})_3(Fe^{3+},Fe^{2+},Ti)(Si_2O_7)_2O_8$—a new chevkinite-group mineral from the Eifel area, Germany. Novye Dannye o Mineralakh, 47, 33–42.

de Hoog, J.C.M., and van Bergen, M.J. (2000) Volatile-induced transport of HFSE, REE, Th and U in arc magmas: evidence from zirconolite-bearing vesicles in potassic lavas of Lewotolo volcano (Indonesia). Contributions to Mineralogy and Petrology, 139, 485–502.

De Paolo, D.J., Manton, W.I., Grew, E.S., and Halpern, M. (1982) Sm-Nd, Rb-Sr and U-Th-Pb systematics of granulite facies rocks from Fyfe Hills, Enderby Land, Antarctica. Nature, 298, 614–618.

Della Ventura, G., Williams, C.T., Raudsepp, M., Bellatreccia, F., Caprilli, E., and Giordano, G. (2001) Perrierite-(Ce) and zirconolite from syenitic ejectum of the Roccamonfina volcano (Latium, Italy): implications for the mobility of Zr, Ti and REE in volcanic environments. Neues Jahrbuch für Mineralogie Monatshefte, 2001, 385–402.

Dickson, J.S. (2015) Rare earth elements: Global market overview. In G.J. Simandl and M. Neetz, Eds., Symposium on Strategic and Critical Materials Proceedings, November 13-14 (2015) Victoria, British Columbia. British Columbia Ministry of Energy and Mines. British Columbia Geological Survey Paper 2015-3, 5–11.

Doelter, C. (1931) Handbuch der Mineralchemie, vol. 3. Steinkopff, Dresden.

Els, F. (2014) Canada wants 20% of global rare earth market by 2018. https://www.mining.com, Jan. 8, 2014 (http://www.mining.com/canada-wants-20-of-global-rare-earth-market-by-2018-27834/; accessed 10 February 2017).

Ewart, A. (1981) The mineralogy and chemistry of the anorogenic Tertiary silicic volcanics of S.E. Queensland and N.E. New South Wales, Australia. Journal of Geophysical Research, 86, 10242–10256.

Goto, A., Kunugiza, K., and Miyajima, H. (2017) Phase relations in the $NaAlSiO_4$-SiO_2-H_2O system for the hydrothermal precipitation of jadeite, albite, natrolite, and analcime in jadeitite of the Itoigawa-Omi area, Japan. Journal of the Mineralogical and Petrological Sciences, 112, 271–280.

Gottardi, G. (1960) The crystal structure of perrierite. American Mineralogist, 45, 1–14.

Green, T.H., and Pearson, N.J. (1988) Experimental crystallization of chevkinite/perrierite from REE-enriched silicate liquids at high pressure and temperature. Mineralogical Magazine, 52, 113–120.

Grew, E.S., and Manton, W.I. (1979a) Archean rocks in Antarctica: 2.5-billion-year uranium-lead ages of pegmatites in Enderby Land. Science, 206, 443–445.

——— (1979b) Geochronologic studies in East Antarctica; age of a pegmatite in Mawson charnockite. Antarctic Journal of the United States, 14, 2–3.

——— (1986) A new correlation of sapphirine granulites in the Indo-Antarctic metamorphic terrain; late Proterozoic dates from the Eastern Ghats province of India. Precambrian Research, 33, 123–137.

Haggerty, S.E., and Mariano, A.N. (1983) Strontian-loparite and strontio-chevkinite: Two new minerals in rheomorphic fenites from the Parana Basin carbonatites, South America. Contributions to Mineralogy and Petrology, 84, 365–381.

Haque, N., Hughes, A., Lim, S., and Vernon, C. (2014) Rare earth elements: Overview of mining, mineralogy, uses, sustainability and environmental impact. Resources, 3, 614–635.

Harley, S.L. (1994) Mg-Al yttrian zirconolite in a partially melted sapphirine granulite, Vestfold Hills, East Antarctica. Mineralogical Magazine, 58, 259–269.

——— (2008) Refining the P-T records of UHT crustal metamorphism. Journal of Metamorphic Geology, 26, 125–154.

Harley, S.L., and Christy, A.G. (1995) Titanium-bearing sapphirine in a partially melted aluminous granulite xenolith, Vestfold Hills, Antarctica. European Journal of Mineralogy, 7, 637–653.

Harlov, D.E. (2015) Apatite: a fingerprint for metasomatic processes. Elements, 11, 171–176.

Harlov, D.E., and Hetherington, C.J. (2010) Partial high-grade alteration of monazite using alkali-bearing fluids: Experiment and nature. American Mineralogist, 95, 1105–1108.

Harlov, D.E., Wirth, R., and Hetherington, C.J. (2011) Fluid-mediated partial alteration in monazite: the role of coupled dissolution-reprecipitation in element redistribution and mass transfer. Contributions to Mineralogy and Petrology, 162, 329–348.

Hirtopanu, P., Andersen, J.C., Fairhurst, R.J., and Jakab, G. (2013) Allanite-(Ce) and its associations, from the Ditrau intrusive massif, East Carpathians, Romania. Proceedings of the Romanian Academy, Series B, 59–74.

Hoatson, D.M., Jaireth, S., and Miezitis, Y. (2011) The major rare-earth-element deposits of Australia.: geological setting, exploration, and resources. Geoscience Australia, 204 pp.

Hokada, T. (2007) Perrierite in sapphirine-quartz gneiss: geochemical and geochronological features and implications for accessory-phase paragenesis of UHT metamorphism. Journal of Mineralogical and Petrological Sciences, 102, 44–49.

Holtstam, D., Bindi, L., Hålenius, U., and Andersson, U.B. (2017) Delhuyarite-(Ce)—$Ce_4Mg(Fe_2^{3+}W)\square(Si_2O_7)_2O_6(OH)_2$—a new mineral of the chevkinite group, from the Nya Bastnäs Fe-Cu-REE deposit, Sweden. European Journal of Mineralogy, 29, 897–905.

Hughes, J.M., and Rakovan, J.F. (2015) Structurally robust, chemically diverse: apatite and apatite supergroup minerals. Elements, 11, 165–170.

Huraiová, M., Konečný, P., and Hurai, V. (2007) Chevkinite-(Ce)—REE-Ti silicate from syenite xenoliths in the Pinciná basaltic maar near Lučenec (Southern Slovakia). Mineralia Slovaca, 39, 255–268 (in Slovak, with English summary).

Imaoka, T., and Nakashima, K. (1994) Chevkinite in syenites from Cape Ashizuri, Shikoku Island, Japan. Neues Jahrbuch für Mineralogie Monatshefte, 1994 (8), 358–366.

Ito, J., and Arem, J.E. (1971) Chevkinite and perrierite: synthesis, crystal growth, and polymorphism. American Mineralogist, 56, 307–319.

Jaffe, H.W., Evans, H.T., and Chapman, R.W. (1956) Occurrence and age of chevkinite from the Devil's Slide fayalite-quartz syenite near Stark, New Hampshire. American Mineralogist, 41, 474–487.

Jiang, N. (2006) Hydrothermal alteration of chevkinite-(Ce) in the Shuiquangou syenitic intrusion, northern China. Chemical Geology, 227, 100–112.

Johnson, T.E., Hudson, N.F.C., and Droop, G.T.R. (2003) Evidence for a genetic granite-migmatite link in the Dalradian of NE Scotland. Journal of the Geological Society London, 160, 447–457.

Jørgensen, K.A. (1980) The Thorsmörk ignimbrite: an unusual comenditic pyroclastic flow in southern Iceland. Journal of Volcanology and Geothermal Research, 8, 7–22.

Kartashov, P.M. (1994) Zr- and Nb-bearing varieties of chevkinite-(Ce) and their alteration products, first occurrence in Mongolia. Ninth IAGOD Symposium (Beijing), 2, 696–697 (abstract).

Kasatkin, A.W., Epanczincev, S.G., and Niestola, F. (2015) Dingdaohengite-(Ce) from Obuhovskovo Uwala, south Urals—first find in Russia. Mineralogy, Yiming Urb RAS., no. 3, 3–7 (in Russian).

Kopylova, M.G., Gurney, J.J., and Daniels, L.R.M. (1997a) Mineral inclusions in diamonds from the River Ranch kimberlite, Zimbabwe. Contributions to Mineralogy and Petrology, 129, 366–384.

Kopylova, M.G., Rickard, R.S., Kleyenstucher, A., Taylor, W.R., Gurney, J.J., and Daniels, L.R.M. (1997b) First occurrence of strontian K-Cr loparite and Cr-chevkinite in diamonds. Russian Geology and Geophysics, 38, 405–420.

Kudrin, V.S., Kudrina, M.A., and Moreyeva, N.V. (1967) Tantalum-niobium mineralisation in lime skarns. Doklady Akademii Nauk SSSR, 177, 430–432 (in Russian).

Lacroix, A. (1915) La bastnaésite et la tscheffkinite de Madagascar. Bulletin de la Société Française de Minéralogie, 38, 106–114.

Li, X.-C., and Zhou, M.-F. (2017) Hydrothermal alteration of monazite-(Ce) and chevkinite-(Ce) from the Sin Quyen Fe-Cu-LREE-Au deposit, northwestern Vietnam. American Mineralogist, 102, 1525–1541.

——— (2018) The nature and origin of hydrothermal REE mineralization in the Sin Quyen deposit, northwestern Vietnam. Economic Geology, 113, 645–673.

Li, G., Yang, G., Ma, Z., Shi, N., Xiong, M., Fan, H., and Sheng, G. (2005) Crystal structure of natural non-metamict Ti- and Fe^{2+}-rich chevkinite-(Ce). Acta Geologica Sinica, 79, 325–331.

Liu, Y., and Ma, C. (2015) Monazite, chevkinite-perrierite and xenotime in martian breccia meteorite NWA 7034. 46th Lunar and Planetary Science Conference 2015, 1287. http://www.hou.usra.edu/meetings

Liu, Y., Ma, C., Beckett, J., and Guan, Y. (2015) Rare-earth minerals in martian meteorite NWA 7034/7533: evidence for fluid-rock interaction in the martian crust. 78th Annual Meeting of the Meteoritical Society, p. 5051.

Liu, Y., Ma, C., Beckett, J.R., Chen, Y., and Guan, Y. (2016) Rare-earth-element minerals in martian breccia meteorites NWA 7034 and 7533: Implications for fluid-rock interaction in the martian crust. Earth and Planetary Science Letters, 451, 252–262.

Lyalina, L.M., Zozulya, D.R., Savchenko, Ye.E., Tarasov, M.P., Selivanova, E.A., and Tarasova, E. (2014) Fluorbritholite-(Y) and yttrialite-(Y) from silexites of the Keivy alkali granites, Kola Peninsula. Geology of Ore Deposits, 56, 589–602.

Macdonald, R., and Belkin, H.E. (2002) Compositional variation in minerals of the chevkinite group. Mineralogical Magazine, 66, 1075–1098.

Macdonald, R., Marshall, A.S., Dawson, J.B., Hinton, R.W., and Hill, P.G. (2002) Chevkinite-group minerals from salic volcanic rocks of the East African Rift. Mineralogical Magazine, 66, 287–299.

Macdonald, R., Belkin, H.E., Wall, F., and Bagiński, B. (2009) Compositional variation in the chevkinite group: new data from igneous and metamorphic rocks. Mineralogical Magazine, 73, 777–796.

Macdonald, R., Bagiński, B., Kartashov, P., Zozulya, D., and Dzierżanowski, P. (2012) Chevkinite-group minerals from Russia and Mongolia: new compositional data from fenites, metasomatites and ore deposits. Mineralogical Magazine, 76, 535–549.

Macdonald, R., Bagiński, B., Dzierżanowski, P., Fettes, D.J., and Upton, B.G.J. (2013) Chevkinite-group minerals in UK Palaeogene granites: underestimated REE-bearing accessory phases. Canadian Mineralogist, 51, 333–347.

Macdonald, R., Sumita, M., Schmincke, H.-U., Bagiński, B., White, J.C., and Ilnicki, S.S. (2015a) Peralkaline felsic magmatism at the Nemrut volcano, Turkey: impact of volcanism on the evolution of Lake Van (Anatolia) IV. Contributions to Mineralogy and Petrology, 169, 34.

Macdonald, R., Bagiński, B., Kartashov, P.M., Zozulya, D., Dzierżanowski, P., and Jokubauskas, P. (2015b) Hydrothermal alteration of a chevkinite-group mineral to a bastnäsite-(Ce)-ilmenite-columbite-(Fe) assemblage: interaction with a F-, CO_2-rich fluid. Mineralogy and Petrology, 109, 659–678.

Macdonald, R., Bagiński, B., Kartashov, P.M., Zozulya, D., and Dzierżanowski, P. (2015c) Hydrothermal alteration of chevkinite-group minerals. Part 2. Metasomatite from the Keivy massif, Kola Peninsula, Russia. Mineralogical Magazine, 79, 1039–1059.

——— (2015d) Interaction of rare-metal minerals with hydrothermal fluids: evidence from quartz-epidote metasomatites of the Haldzan Buragtag massif, Mongolian Altai. Canadian Mineralogist, 55, 1015–1034.

Macdonald, R., Nejbert, K., Bagiński, B., and Jurewicz, E. (2017a) Ti-Zr-Nb-bearing accessory minerals in high-K trachyandesitic rocks from the Western Outer Carpathians, Moravia, Czech Republic. European Journal of Mineralogy, 30, 135–147.

Macdonald, R., Bagiński, B., and Zozulya, D. (2017b) Differing responses of zircon, chevkinite-(Ce), monazite-(Ce) and fergusonite-(Y) to hydrothermal alteration: Evidence from the Keivy alkaline province, Kola Peninsula, Russia. Mineralogy and Petrology, 111, 523–545.

Makagonov, E.P., and Muftakhov, V.A. (2016) REE and Sr mineralization with perrierite-(Ce) in alkaline silicate—carbonate assemblage of the contact zone of the Vishnevogorsk Block (South Urals). Mineralogy, No. 4, 19–30 (in Russian).

Makarochkin, B.A., Gonibesova, K.A., and Makarochkina, M.S. (1959) Chevkinite from the Ilmen Mountains. Zapiski Vserossiiskogo Mineralogicheskogo Obshchestva USSR, 88, 547–553 (in Russian).

Marchenko, Ye.-Ya., Chashka, A.I., and Gurova, Ye.P. (1968) The substitution of chevkinite by bastnesite under the conditions of a carbonate-halide hydrothermal process. Dopovidi Akademiyi Nauk Ukrayins'koyi RSR, Seriya B: Geologichni, Khimichni ta Biologichni Nauki, 1, 69–72 (in Ukrainian).

Marshall, A.S., Macdonald, R., Rogers, N.W., Fitton, J.G., Tindle, A.G., Nejbert, K., and Hinton, R.W. (2009) Fractionation of peralkaline silicic magmas: the Greater Olkaria Volcanic Complex, Kenya Rift Valley. Journal of Petrology, 50, 323–359.

Martin, H., Bonin, B., Capdevila, R., Jahn, B.M., Lameyre, J., and Wang, Y. (1994) The Kuiqi peralkaline granitic complex (SE China): petrology and geochemistry. Journal of Petrology, 35, 983–1015.

Martz, A.M., and Brown, F.H. (1981) Chemistry and mineralogy of some Plio-Pleistocene tuffs from the Shungura Formation, southwest Ethiopia. Quaternary Research, 16, 240–257.

Mashima, H., Akai, J., Nakamuta, Y., and Matsubara, S. (2008) Orthorhombic polymorph of rengeite from Ohmi region, central Japan. American Mineralogist, 93, 1153–1157.

McDowell, S.D. (1979) Chevkinite from the Little Chief Granite porphyry stock, California. American Mineralogist, 64, 721–727.

Melluso, L., Hergt, J.M., and Zanetti, A. (2014) The late crystallization stages of low-Ti, low-Fe tholeiitic magmas: Insights from evolved Antarctic and Tasmanian rocks. Lithos, 188, 72–83.

Mikhailova, Yu.A., Konopleva, N.G., Yakovenchuk, V.N., Ivanyuk, G.Yu., Men'shikov, Yu.P., and Pakhomovsky, Ya.A. (2007) Corundum-group minerals in rocks of the Khibiny alkaline pluton, Kola Peninsula. Geology of Ore Deposits, 49, 590–598.

Mills, J.G., Saltoun, B.W., and Vogel, T.A. (1997) Magma batches in the Timber Mountain magmatic system, Southwestern Nevada Volcanic Field, Nevada, USA. Journal of Volcanology and Geothermal Research, 78, 185–208.

Mills, S.J., Kartashov, P.M., Kampf, A.R., Konev, A.A., Koneva, A.A., and Raudsepp, M. (2012) Cordylite-(La), a new mineral species in fenite from the Biraya Fe-REE deposit, Irkutsk, Russia. Canadian Mineralogist, 50, 1281–1290.

Min, K., Reiners, P.W., Wolff, J.A., Mundil, R., and Winters, R.L. (2006) (U-Th)/He dating of volcanic phenocrysts with high-U-Th inclusions, Jemez Volcanic Field, New Mexico. Chemical Geology, 227, 223–235.

Mineev, D.A., Makarochkin, B.A., and Zhabin, A.G. (1962) The study of lanthanide behaviour in alteration processes of rare-earth minerals. Geokhimiya, 7, 590–597 (in Russian).

Mitchell, R.S., Swanson, S.M., and Crowley, J.K. (1976) Mineralogy of a deeply weathered pegmatite, Bedford County, Virginia. Southeastern Geology, 18, 37–47.

Miyajima, H., Matsubara, S., Miyawaki, R., Yokoyama, K., and Hirokawa, K. (2001) Rengeite, $Sr_4ZrTi_4Si_4O_{22}$, a new mineral, the Sr-Zr analogue of perrierite from the Itoigawa-Ohmi district, Niigata prefecture, central Japan. Mineralogical Magazine, 65, 111–120.

Miyajima, H., Miyawaki, R., and Ito, K. (2002) Matsubaraite, $Sr_4Ti_5(Si_2O_7)_2O_8$, a new mineral, the Sr-Ti analogue of perrierite in jadeitite from the Itoigawa-Ohmi district, Niigata prefecture, Japan. European Journal of Mineralogy, 14, 1119–1128.

Miyawaki, R., Matsubara, S., and Miyajima, H. (2002) The crystal structure of rengeite, $Sr_4ZrTi_4(Si_2O_7)O_8$. Journal of Mineralogical and Petrological Sciences, 97, 7–12.

Miyawaki, R., Matsubara, S., Yokoyama, K., Momma, K., Sano, T., Tsutsumi, Y., Shigeoka, M., and Nishikubo, K. (2012) Chevkinite-(Ce) in tuff at Heguri, Boso Peninsula, Chiba Prefecture, Japan. Bulletin of the National Museum of Natural Sciences, Ser. C, 38, 7–13.

Miyazaki, T., and Santosh, M. (2005) Cooling history of the Putetti alkali syenite pluton, southern India. Gondwana Research, 8, 567–574.

Monchoux, P., Fontan, F., de Parseval, P., Martin, R.F., and Wang, R.C. (2006) Igneous albitite dikes in orogenic lherzolites, Western Pyrénées, France: a possible source for corundum and alkali feldspar xenocrysts in basaltic terranes. 1. Mineralogical Associations. Canadian Mineralogist, 44, 817–842.

Montel, J.M. (1986) Experimental determination of the solubility of Ce-monazite in SiO_2-Al_2O_3-K_2O-Na_2O melts at 800°C, 2 kbar, under H_2O-saturated conditions. Geology, 14, 659–662.

——— (1993) A model for monazite/melt equilibrium and application to the generation of granitic magmas. Chemical Geology, 110, 127–146.

Muhling, J.R., Suvorova, A.A., and Rasmussen, B. (2014) The occurrence and composition of chevkinite-(Ce) and perrierite-(Ce) in tholeiitic intrusive rocks and lunar mare basalt. American Mineralogist, 99, 1911–1921.

Mutanen, T. (1997) Geology and ore petrology of the Akanvaara and Koitelainen mafic layered intrusions and the Keivitsa-Satovaara layered complex, northern Finland. Geological Survey of Finland, Bulletin, 395, 233 pp.

Nespolo, M., Ferraris, G., and Ohasi, H. (1999) Charge distribution as a tool to investigate structural details: meaning and application to pyroxenes. Acta Crystallographica, B55, 902–916.

Noble, D.C. (1965) Gold Flat Member of the Thirsty Canyon Tuff—a pantellerite ash-flow sheet in southern Nevada. U.S. Geological Survey Professional Paper 525-B, B85–B90.

Novak, S.W., and Mahood, G.A. (1986) Rise and fall of a basalt-trachyte-rhyolite magma system at the Kane Springs Wash Caldera, Nevada. Contributions to Mineralogy and Petrology, 94, 352–373.

Ontoyev, D. (1993) Ore-bearing metasomatites at the Bayan Obo rare earth deposit, Inner Mongolia, China. International Geology Review, 35, 271–278.

Padilla, A.J., and Gualda, G.A.R. (2016) (2016) Crystal-melt elemental partitioning in silicic magmatic systems: An example from the Peach Spring Tuff high-silica rhyolite, Southwest USA. Chemical Geology, 440, 326–344.

Papoutsa, A.D., and Pe-Piper, G. (2013) The relationship between REE-Y-Nb-Th minerals and the evolution of an A-type granite, Wentworth Pluton, Nova Scotia. American Mineralogist, 98, 444–462.

Parodi, G.C., Della Ventura, G., Mottana, A., and Raudsepp, M. (1994) Zr-rich non metamict perrierite-(Ce) from holocrystalline ejecta in the Sabatini volcanic complex (Latium, Italy). Mineralogical Magazine, 58, 607–613.

Payette, C., and Martin, R.F. (1988) The Welsford anorogenic igneous complex, southern New Brunswick: rift-related Acadian magmatism. Geological Survey of Canada Open File 1727.

Peretyazhko, I.S., Savina, E.A., and Karmanov, N.S. (2015) Comendites and pantellerites of Nemrut volcano, Eastern Turkey: genesis and relations between the trachyte-comendite, comenditic, and pantelleritic melts. Petrology, 23, 576–622.

Pin, C., Monchoux, P., Paquette, J.-L., Azambre, B., Wang, R.C., and Martin, R.F. (2006) Igneous albitite dikes in orogenic lherzolites, western Pyrénées, France: a possible source for corundum and alkali feldspar xenocrysts in basaltic terranes. II. Geochemical and petrogenetic considerations. Canadian Mineralogist, 44, 843–856.

Popov, V.A., Pautov, L.A., Sokolova, E., Hawthorne, F.C., McCammon, C., and Bazhenova, L.F. (2001) Polyakovite-(Ce), $(REE,Ca)_4(Mg,Fe^{2+})(Cr^{3+},Fe^{3+})_2(Ti,Nb)_2Si_4O_{22}$, a new metamict mineral species from the Ilmen Mountains, southern Urals, Russia: mineral description and crystal chemistry. Canadian Mineralogist, 39, 1095–1104.

Portnov, A.M. (1964) Strontium perrierite in the North Baikal region. Doklady of the Academy of Sciences USSR: Earth Science Section, 156, 118–120.

Povarennykh, O.S., and Ganzeeva, L.V. (1972) Manganous chevkinite from alkaline metasomites of the Russian Platform. Dopodivi Akademiyi Nauk Ukrayins'koyi RSS Seriya B: Geologichni, Khimichni ta Biologichni Nauki, 9, 794–797 (in Russian).

Prol-Ledesma, R.-M., Melgarejo, J.C., and Martin, R.F. (2012) The El Muerto "NYF" granitic pegmatite, Oaxaca, Mexico, and its striking enrichment in allanite-(Ce) and monazite-(Ce). Canadian Mineralogist, 50, 1055–1076.

Proshchenko, Ye.G. (1967) Rare earth minerals from albitites of eastern Siberia, p. 103–136 Mineralogiya pegmatitov i gidrotermalitov shchelochnykh massivov. Akademii Nauk SSSR, Institut Mineralogii, Geokhimii, Kristallokhimii Redk. Elementov, Moscow (in Russian).

Rajesh, H.M. (2003) Outcrop-scale silicate liquid immiscibility from an alkali syenite (A-type granitoid)-pyroxenite association near Puttetti, Trivandrum Block, South India. Contributions to Mineralogy and Petrology, 145, 612–627.

Rapp, R.P., Ryerson, F.J., and Miller, C.F. (1987) Experimental evidence bearing on the stability of monazite during crustal anatexis. Geophysical Research Letters, 14, 307–310.

Rasmussen, B., Fletcher, I.R., Gregory, C.J., and Muhling, J.R. (2014) Six chronometers in one rock: Dating mafic intrusive rocks by in situ SHRIMP U-Pb geochronology. Goldschmidt Abstracts 2034.

Ridolfi, F., Renzulli, A., Santi, P., and Upton, B.G.J. (2003) Evolutionary stages of crystallization of weakly peralkaline syenites: evidence from ejecta in the plinian deposits of Agua de Pau volcano (São Miguel, Azores Islands). Mineralogical Magazine, 67, 749–767.

Robinson, D., and Miller, C. (1999) Record of magma chamber processes preserved in accessory mineral assemblages. American Mineralogist, 84, 1346–1353.

Rozanov, K.I., Flerova, L.B., Khomich, P.Z., and Zingerman, A.Ya. (1983) Fractionation and concentration of lanthanides and ytrrium in Precambrian complexes of the western part of the Russian platform. Doklady, Academy of Sciences of the USSR, Earth Sciences Section, 258, 177–181.

Savel'eva, V.B., and Karmanov, N.S. (2008) REE minerals of alkaline metasomatic rocks in the Main Sayan Fault. Geology of Ore Deposits, 50, 681–696.

——— (2010) Quartz-albite-microcline metasomatic rocks in the Main Sayan Fault Zone: Evolution of metasomatism and composition of accessory minerals. Geology of Ore Deposits, 52, 302–321.

Sawyer, D.A., and Sargent, K.A. (1989) Petrologic evolution of divergent peralkaline magmas from the Silent Canyon caldera complex, southwestern Nevada volcanic field. Journal of Geophysical Research, 94, 6021–6040.

Scaillet, B., and Macdonald, R. (2001) Phase relations of peralkaline silicic magmas and petrogenetic implications. Journal of Petrology, 42, 825–845.

Segelstad, T.V., and Larsen, A.O. (1978) Chevkinite and perrierite from the Oslo region, Norway. American Mineralogist, 63, 499–505.

Semenov, E.I., Kulakov, M.P., Kostynina, L.P., Kazakova, M.E., and Dudykina, A.S. (1966) Scandium content in the quartz-fluorite pegmatites of Kazakhstan. Geokhimiya, 2, 244–246.

Semenov, E.I., Upendran, R., and Subramanian, V. (1978) Rare earth minerals of carbonatites of Tamil Nadu. Journal of the Geological Society of India, 19, 550–557.

Shellnutt, J.G., and Iizuka, Y. (2013) Chevkinite-group minerals from the mantle-derived metaluminous Woshui syenite of the Emeishan large igneous province. European Journal of Mineralogy, 25, 671–682.

Shen, G., Yang, G., and Xu, J. (2005) Maoniupingite-(Ce): A new rare-earth mineral from the Maoniuping rare-earth deposit in Mianning, Sichuan, China. Sedimentary Geology and Tethyan Geology, 25, 210–216 (in Chinese with English abstract).

Shimazaki, H., Yang, Z., Miyawaki, R., and Shigeoka, M. (2008a) Scandium-bearing

minerals in the Bayan Obo Nb-REE-Fe deposit, Inner Mongolia, China. Resource Geology, 58, 80–86.
Shimazaki, H., Miyawaki, R., Yokoyama, K., Matsubara, S., Yang, Z., and Shigeoka, M. (2008b) A reconnaissance study on minerals from the Bayan Obo Nb-REE-Fe deposit, Inner Mongolia, China. Bulletin of the National Museum of Nature and Science, 34, 1–26.
Smith, M.P., Moore, K., Kavecsánszki, D., Finch, A.A., Kynicky, J., and Wall, F. (2016) From mantle to critical zone: A review of large and giant sized deposits of the rare earth elements. Geoscience Frontiers. doi: 10.1016/j.gsf.2015.12.006.
Sokolova, E., Hawthorne, F.C., Della Ventura, G., and Kartashov, P.M. (2004) Chevkinite-(Ce): crystal structure and the effect of moderate radiation-induced damage on site-occupancy refinement. Canadian Mineralogist, 42, 1013–1025.
Stachowicz, M., Bagiński, B., Macdonald, R., Kartashov, P.M., Oziębło, A., and Woźniak, K. (2014) Structure of Sr-Zr-bearing perrierite-(Ce) from the Burpala Massif, Russia. Mineralogical Magazine, 78, 1647–1659.
Stachowicz, M., Bagiński, B., Welch, M.D., Kartashov, P.M., Macdonald, R., Balcerzak, J., Tyczkowski, J., and Woźniak, K. (2019) Cation ordering, valence states and symmetry breaking in the crystal-chemically complex mineral chevkinite-(Ce), X-ray diffraction and photoelectron spectroscopy studies, and mechanisms of Nb enrichment. American Mineralogist, 104, in press.
Troll, V.R., Sachs, P.M., Schmincke, H.-U., and Sumita, M. (2003) The REE-Ti mineral chevkinite in comenditic magmas from Gran Canaria, Spain: a SYXRF-probe study. Contributions to Mineralogy and Petrology, 145, 730–741.
van Bergen, M.J. (1984) Perrierite in siliceous lavas from Mt Amiata, central Italy. Mineralogical Magazine, 48, 553–556.
Vasquez, J.A. (2008) Allanite and chevkinite as absolute chronometers of rhyolite differentiation. Geological Society of America Abstracts with Programs, 40, 74.
Vasquez, J.A., Manning, C.E., and Reid, M.R. (2004) Experimental determination of allanite stability in high-silica rhyolite. American Geophysical Union, Fall Meeting 2004, abstract V41C-1407.
Vasquez, J.A., Kyriazis, S.F., Reid, M.R., Sehler, R.C., and Ramos, F.C. (2009) Thermochemical evolution of young rhyolites at Yellowstone: Evidence for a cooling but periodically replenished postcaldera magma reservoir. Journal of Volcanology and Geothermal Research, 188, 186–196.
Vasquez, J.A., Velasco, N.O., Schmitt, A.K., Bleick, H.A., and Stelten, M.E. (2014) ^{238}U-^{230}Th dating of chevkinite in high-silica rhyolites from La Primavera and Yellowstone calderas. Chemical Geology, 390, 109–118.
Vasyukova, O., and Williams-Jones, A.E. (2016) The evolution of immiscible silicate and fluoride melts: Implications for REE ore-genesis. Geochimica et Cosmochimica Acta, 172, 205–224.
Viladkar, S.G., Sorokhtina, N.V., and Senin, V.G. (2009) The Zr-Ti mineralization in carbonatites of the Samchampi alkaline carbonatite complex, Assam, India. http://geo.web.ru/conf/alkaline/2009/Viladkar.htm
Vlach, S.R.F., and Gualda, G.A.R. (2007) Allanite and chevkinite in A-type granites and syenites of the Graciosa Province southern Brazil. Lithos, 97, 98–121.
Wang, D., Yang, J., Yan, S., Xu, J., Chen, Y., Pu, G., and Luo, Y. (2001) A special orogenic-type rare earth element deposit in Maoniuping, Sichuan, China: geology and geochemistry. Resource Geology, 51, 177–188.
Warren, G.R., Byers, F.M., Broxton, D.E., Freeman, S.H., and Hagan, R.C. (1989) Phenocryst abundance and glass and phenocryst compositions as indicators of magmatic environments of large-volume ash flow sheets in southwestern Nevada. Journal of Geophysical Research, 94, 5987–6020.
Wu, B., Wang, R.-C., Yang, J.-H., Wu, F.-Y., Zhang, W.-L., Gu, X.-P., Zhang, A.-C. (2016) Zr and REE mineralization in sodic lujavrite from the Saima alkaline complex, northeastern China: A mineralogical study and comparison with potassic rocks. Lithos, 262, 232–246.
Xu, J., Yang, G., Li, G., Wu, Z., and Shen, G. (2008) Dingdaohengite-(Ce) from the Bayan Obo REE-Nb-Fe Mine, China: Both a true polymorph of perrierite-(Ce) and a titanic analog at the C1 site of chevkinite subgroup. American Mineralogist, 93, 740–744.
Yakovenchuk, V.N., Ivanuyk, G.Yu., Pakhomovsky, Ya.A., and Menshikov, Yu.P. (2005) Khibiny. In F. Wall, Ed., Laplandia Minerals, Apatity. Mineralogical Society of Great Britain and Ireland, 468 pp.
Yang, Z., Fleck, M., Smith, M., Tao, K., Song, R., and Zhang, P. (2002) The crystal structure of natural Fe-rich chevkinite. European Journal of Mineralogy, 14, 969–975.
Yang, Z., Li, H., Liu, M., and Franz, P. (2007) Crystal chemistry of iron in non-metamict chevkinite-(Ce): valence state and site occupation proportions. Journal of Rare Earths, 25, 238–242.
Yang, Z., Pertlik, F., and Fleck, M. (2008) Hydroxyl groups in nonmetamict chevkinite-(Ce): a crystal chemical discussion. Journal of Rare Earths, 26, 609–613.
Yang, Z., Giester, G., Ding, K., and Tillmanns, E. (2012) Hezuolinite, $(Sr,REE)_4Zr(Ti,Fe^{3+},Fe^{2+})_2Ti_2O_8(Si_2O_7)_2$, a new mineral species of the chevkinite group from Saima alkaline complex, Liaoning Province, NE China. European Journal of Mineralogy, 24, 189–196.
Zhang, R., and Long, Z. (1987) The discovery of chevkinite from the alkali-granites in southwestern Sichuan. Journal of Chengdu College of Geology, 14, 61–64.
Zozulya, D., and Eby, G.N. (2010) Rare-metal ore occurrences, related to the late Archean A-type granites from the Keivy zone (NE Fennoscandian shield). In O.T. Raino, S.R. Lukkari, and A.P. Heinanen, Eds., International Conference on A-type granites and related rocks through time (IOCP-510), Helsinki, Finland, August 18–20. Abstract volume, 113–115.

Manuscript received August 3, 2018
Manuscript accepted November 27, 2018
Manuscript handled by Daniel Harlov

Endnote:

[1]Deposit item AM-19-36772, Supplemental Material and Tables. Deposit items are free to all readers and found on the MSA website, via the specific issue's Table of Contents (go to http://www.minsocam.org/MSA/AmMin/TOC/2019/Mar2019_data/Mar2019_data.html).